Application of Hilbert transform to scalp EEG containing EMG

Human Brain Mapping 19(4):248-272

Walter J Freeman*

Brian C Burke
Department of Molecular & Cell Biology, LSA 142
University of California
Berkeley CA 94720-3200 USA
tel: 510-642-4220 fax: 510-643-6791
wfreeman@socrates.berkeley.edu
burkeb@uclink.berkeley.edu

Mark D Holmes
EEG & Clinical Neurophysiology Laboratory
325 Ninth Ave, Harborview Medical Center
Box 359722, Seattle, WA 98104
tel: 206-731-3502 fax: 206-731-8545
mdholmes@u.washington.edu
*Corresponding author

29 January 2003 56 pages 13,449 words 19 figures

Key Words: analytic phase, EEG, EMG, Hilbert transform, neurodynamics, state transition, scalp EEG

Acknowledgments

The human data were collected by Mark D. Holmes and Sampsa Vanhatalo in the EEG & Clinical Neurophysiology Laboratory, Harborview Medical Center, Seattle WA. The linear electrode array was constructed by Anthony Bell in accordance with a Berkeley design. Programming was done in the Division of Neurobiology at Berkeley by Brian C. Burke. Editorial assistance from Sampsa Vanhatalo and discussions with Linda Rogers, J. Kurths of Uni-Potsdam, Steve Kercel of Oak Ridge TN, and Ceon Ramon of Seattle are gratefully acknowledged. Partial support was provided through a grant NCC 2-1244 from NASA and a grant EIA-0130352 from NSF.

Abstract

Objective: To evaluate rapid changes in regional EEG synchronization in normal subjects with spatial and temporal resolution exceeding prior art 10-fold.
Methods: A curvilinear array of 64 electrodes 3 mm apart extending 18.9 cm across the scalp was used to record EEG at 200/s. Analytic amplitude (AA) and phase (AP) were calculated at each time step for the 64 traces in the analog pass band of 0.5-120 Hz. AP differences approximated the AP derivative (instantaneous frequency). The AP from unfiltered EEG revealed no reproducible patterns. Filtering was necessary in the beta and gamma ranges according to a technique that optimized the correlation of the AP differences with the activity band pass filtered in the alpha range.
Results: The sizes of temporal AP differences were usually within ±0.5 radian from the average step corresponding to the center frequency of the pass band. Large AP differences were often synchronized over distances of 6 to 19 cm. An optimal pass band to detect and measure these recurring jumps in AP in the beta and gamma ranges was found by maximizing the alpha peak in the cospectrum of the correlation between unfiltered EEG and the band pass AP differences. Synchronized AP jumps recurred in clusters (CAP) at alpha rates in resting subjects and with EMG.
Conclusion: Cortex functions by serial changes in state. The Hilbert transform of EEG from high density arrays can visualize these state transitions with high temporal and spatial resolution and should be useful in relating EEG to cognition.

Introduction

The genesis and control of behavior requires the coordination of diverse areas of cerebral cortex interacting with the subcortical structures. Well defined behavioral states require sequential epochs of cortical activity, in which the neural activity in multiple cortical areas is formed by cooperation and expressed in spatial patterns. Studies of intracranial EEG from high density electrode arrays implanted in animals on sensory cortices have revealed episodic spatial patterns of amplitude and phase modulation (AM and PM) of carrier waves in the gamma range (Freeman, 2000a) from primary sensory areas: olfactory (Freeman and Viana Di Prisco 1986; Freeman and Grajski 1987), visual (Freeman and van Dijk, 1987), auditory (Ohl, Scheich and Freeman, 2001), and somatomotor (Barrie, Freeman and Lenhart 1996). These epochs were denoted "wave packets" (Freeman, 1975). The AM patterns were related to conditioned stimuli (CS) that the animals had been trained to discriminate. The PM had the stereotypic form of a radially symmetric phase gradient. The isophase contours indicated the form of a cone, when phase values were plotted in the two surface dimensions of the cortex. This pattern resembled the spreading wave from a pebble dropped in water. It indicated that the cortical states expressed in AM patterns formed abruptly and replaced prior patterns in rapid succession at rates in the theta and delta ranges (Freeman and Baird 1987; Freeman and Barrie, 2000, Freeman, 2003a). The statistical relation of the patterns to conditioned stimuli indicated that the neural activity manifesting AM patterns was involved in the genesis and control of discriminative behavior.

These results were based on the Fourier transform. The temporal resolution for investigating the manner of pattern change was limited by the necessity for defining the frequency over a time interval long enough to include at least one cycle of each frequency (Freeman, 2003a). This limitation prevented examining rapid changes in phase patterns. The limitation was overcome by using the Hilbert transform (Barlow 1993; Pikovsky et al., 2001), which transforms time series data into a vector by decomposing it into two independent time series, one for the analytic amplitude (AA) and the other for the instantaneous analytic phase (AP). The calculation of phase is modulo π or 2π, so the phase has the appearance of a sawtooth function. For segments of arbitrary duration the phase must be unwrapped to display it as continuously varying with time. The frequency is given by the slope of the function, either in the local vicinity of each digitized value or averaged over any convenient time window. Thus phase is derived before frequency from EEG with high temporal resolution, limited only by the digitizing rate, in contrast to the Fourier method, in which phase follows frequency decomposition with high frequency resolution but poor temporal resolution (Le Van Quyen et al., 2001; Quiroga et al., 2002).

The results from applying the Hilbert method to the animal data (Freeman and Rogers 2002) confirmed the prediction of finding local epochs of stable phase patterns, that were punctuated by abrupt changes in AA and AP in the multiple traces. These abrupt changes together revealed a transition from one state to another state of the cortical dynamics. The sequential AP jumps were approximately synchronized over the recording areas, with directions of change (+ or -) that varied randomly with time and location. This variation was in accord with the formation at each cortical state change of a new phase cone with its apex having a new sign and location. The Hilbert transform made it possible to evaluate the degree of synchrony within an area of cortex, which was based in the stabilization of a non-zero distribution of AP values in a conic pattern. This was done by using an index of pairwise synchrony derived by Tass et al. (1998) from Shannon entropy that was applied to the phase distributions. That index was generalized to multiple traces within each cortical area (Freeman and Rogers, 2002) and then extended to an evaluation of synchrony over traces from multiple cortical areas (Freeman and Rogers, submitted).

The clean separation of the AP and AA by the Hilbert transform appeared suitable for application to human scalp EEG for improved temporal resolution in search of evidence for episodic changes in cortical states that resembled wave packets. However, the AP and AA were not interpretable when the Hilbert transform was applied to noisy, broad band signals from multiple recording sites. The aim of the present study was to apply the Hilbert transform for the analysis of human scalp EEG and evaluate rapid changes in the synchrony between multiple areas of the brain, that is thought to occur during cognitive behavior (Bressler, 1995; Tallon-Baudry et al., 1996, 1998; Miltner et al., 1999; Rodriguez et al., 1999; Lachaux et al., 1999; Haig et al., 2000; Müller et al., 1996; Müller, 2000; Varela et al. 2001).

Methods and their rationales

Subjects were five male and four female adult volunteers, who were asked to sit quietly and relax their muscles, first with eyes closed and then with eyes open. Clean records free of movement artifacts were selected by off-line editing. For comparison, records were also selected in periods of EMG activity deliberately induced by tensing the scalp. The data were collected in the EEG Clinic of Harborview Hospital, University of Washington, Seattle, and were sent by ftp without identifying markers of personal information to the University of California at Berkeley for analysis. The data collection and management were governed by protocols approved by the Helsinki Declaration and the Institutional Review Boards in both institutions.

A curvilinear electrode array was made with 64 gold-plated needles threaded into a band of embroidery fabric with interstices at 3 mm intervals for a length of 18.9 cm. The scalp was cleaned and dried, and the array was bound firmly onto the forehead across the midline just below the frontal hairline, paracentrally along the part line, or across the occiput. Recordings were referential all with respect to the same reference electrode either on the vertex for frontal and occipital recording or on the contralateral mastoid for paracentral recording. The ground was located on the contralateral mastoid for frontal and paracentral recording, and on the frontal midline (AFz) for occipital recording. The EEG were amplified with a Nicolet (BMSI 5000) system having a fixed gain of 1628 and analog filters set at 0.5 Hz high pass and 120 Hz low pass. The ADC gave 12 bits with the least significant bit of 0.9 microvolts and a maximal range 4096 bits. Possible DC amplifier offsets were removed off-line by subtracting the channel means of each entire recording. The digitizing rate was 200 samples/s (5 ms interval), while the analog filter was set at 120 Hz, with the possibility of aliasing between 80-100 Hz. The data for each subject and condition were blocked into matrices of 5000 data points. Temporal power spectral densities (PSD_t) were calculated with the 1-D FFT for every channel after applying a Hanning window to epochs usually of 1 s, nonoverlapping, and ranging from .1 s to the full duration of each block for each of the 64 EEG. The 64 PSD_t were averaged and transformed for display in log-log coordinates.

Most of the data processing was done with MATLAB software, including convolution in the time domain for temporal filtering with finite impulse response (FIR) filters estimated using Parks-McClellan algorithm of order 200. The transition band width was 4 Hz, except in the cases of narrow adjacent temporal filters, where the transition band width was 1 Hz. Special purpose software was developed for spatial filtering (Freeman and Baird, 1987) of the EEG in the spatial frequency domain. The 1-D FFT was applied to the 64 digitized EEG amplitudes at each time point to get the spatial power spectral density (PSD_x). The spectrum was multiplied by an exponential filter, and the inverse FFT was taken of the real and imaginary parts of the spectrum to get the filtered spatial patterns (Freeman, 2000). An exponential low pass filter was used (Gonzalez and Wintz, 1977) with the factor for attenuation, $A(f_x)$, ranging from 1 and 0 with increasing spatial frequency, f_x , by

$$A(f_x) = \exp \{-.347 [(f_x) / f_o]^n \} , \quad (1)$$

where f_o was the cut-off frequency, n = 2. The same equation held for a high pass filter with n = -6 with $A(f_x)$ ranging from 0 to 1 with increasing frequency. The effect on the PSD_x of padding with zeroes was evaluated with standard padding giving twice the data length (128 bins) and then repeating the 1-D FFT first without padding, giving a length of 64 bins, and then with embedding at twice the standard length (256 bins). The standard embedding gave smoother curves with better spatial frequency resolution than did no padding. Longer embedding merely extended the low frequency ends of the spectra and enhanced a ripple at the upper ends without adding information.

Owing to the broad spectral distribution of EEG power, temporal band pass filtering was required prior to application of the Hilbert transform (Le Van Quyen et al. 2001; Quiroga et al., 2002; Pikovsky, Rosenblum and Kurths, 2001; Freeman and Rogers, 2002). An example of a .5 s segment of EEG is shown in Figure 1,A after filtering in the beta band. Each EEG denoted v(t) was transformed to a vector, V(t), having a real part, v(t), and an imaginary part, v'(t),

$$V(t) = v(t) + i\, v'(t) = AA(t) \exp [iAP(t)] \quad (2)$$

where the real part was the same as the EEG, and the imaginary part was given by the Hilbert transform of v(t),

$$v'(t) = 1/\pi\, PV \int_{-\infty}^{+\infty} v(t') / (t - t')\, dt', \quad (3)$$

Where PV meant the Cauchy Principal Value. At each digitizing step the EEG yielded a point in the complex plane representing the tip of a vector (the dots in Figure 1,B). The length of the vector gave the analytic amplitude,

$$AA(t) = [\, v^2(t) + v'^2(t)\,]^{.5}, \quad (4)$$

and arc tangent of the vector gave the analytic phase,

$$AP(t) = \text{atan} [\, v'(t) / v(t)\,]. \quad (5)$$

With elapsed time the vector rotated counter-clockwise, starting at the blue dot and ending at the red dot in this segment. The trajectory described a loop that usually but not always enclosed the origin of the complex plane. The arc tangent was calculated using the two-quadrant inverse tangent function 'atan' or the four-quadrant inverse tangent function 'atan2' (Figure 1,C). The atan ranged from $-\pi/2$ to $\pi/2$ and on reaching $\pi/2$ fell to $-\pi/2$, while the atan2 function of the same data ranged from $-\pi$ to π and on reaching π fell to $-\pi$ with each crossing of the ordinate, the imaginary axis. The resulting time series resembled a sawtooth, with small increments along a diagonal from the lower bound to the upper bound, and an immediate single downward fall to the lower bound on reaching the upper bound. In order to track the AP over arbitrarily long time intervals the disjoint phase sequences were straightened by adding π to the atan function or 2π to the atan2 function at each discontinuity (Figure 1, D). This joining process would better be called offsetting, as the algorithmic solution was to add offsets cumulatively at each disjoint phase resetting.

Single EEG time series as shown in Figure 1 were tractable, but multiple time series were not, even with narrow band pass filtering. A set of 64 unwrapped AP(t) is shown in Figure 2 grouped by color into 4 subsets of 16 adjacent channels. As was usually the case the initial AP values were distributed within $\pm\pi$ about zero. When temporal filtering was omitted (upper frame), the mean rates of increase over the 1250 ms segment (250 steps at 5 ms/step) varied widely from 1 to 13 Hz. The erratic increase in AP with prominent jumps of approximately π radians was typical of that seen with colored noise. The jumps have been called "phase slip" (Pikovsky, Rosenblum and Kurths, 2001). When a band pass filter was applied (12-30 Hz, lower frame), the AP values increased more smoothly. However, the slopes and intercepts varied unpredictably among channels, primarily because the 64 rotating vectors did not all cross the imaginary axis simultaneously with each cycle at the mean frequency, and not all of them crossed on every cycle (Figure 1B). This variation prevented comparisons of the AP values across channels over extended time periods.

Importantly, the local rates of change were not so strongly affected by this variation between channels. Therefore, the temporal AP differences were calculated as time series for each channel. The spatial AP differences between channels were displayed in 3-D graphs with magnitude of AP difference on the ordinate, time on the left abscissa, and distance (channel number) on the right abscissa (Figures 9-10). The phase differences were plotted as absolute values in order to avoid hiding the negative peaks below the surface. The global mean, equivalent to the average slope and the mean frequency over the segment, was subtracted in order to remove the unregulated variance modulo π and emphasize the local deviations in instantaneous frequency about the mean frequency.

Experience with animal data had shown that the direction of change was immaterial. Further enhancement of display was based on an empirical observation that rapid physiological changes in AP tended to occur at many locations nearly simultaneously and to be accompanied by minima of the AA on the same channels. Selective display of the sudden changes in AP that were nearly simultaneous across multiple channels was facilitated by converting the AA to a weight, W,

$$W(t) = 10 \exp (-AA(t)/10). \quad (6)$$

The values of W ranged inversely from near zero for high AA to 1 for zero AA. The absolute de-meaned AP(t) values were multiplied by W(t). This algorithm improved the detection of synchronization among the temporal AP differences by taking advantage of the information in the AA (Figure 14). As shown in Figure 1,C the minima in AA were independent of the zero crossings of the band pass filtered EEG (Freeman et al., 2003).

The salient problem in applying the Hilbert transform to EEG was the choice of the temporal pass band. In prior studies of animal EEG an optimal pass band was chosen by means of a behavioral criterion. The pass band was systematically varied to make tuning curves, and the settings of the upper and lower cut-off frequencies were found at which the rates of correct classification of spatial AM patterns of EEG amplitude were highest (20-80 Hz in rabbits, Barrie, Freeman and Lenhart, 1996; 35-60 Hz in cats, Freeman, Gaál and Jörsten, 2003). The finding emerged from those studies that the correlation of AP phase differences with EEG activity in the theta ranges was also optimized (Freeman and Rogers, 2002). In the absence of an appropriate behavioral measure in the present study, the optimal pass bands for temporal filtering before application of the Hilbert transform were found as follows. Autocorrelations were calculated for each channel averaged over channels in segments 2 s in duration for the raw EEG and the signed temporal AP differences, and so likewise the cross-correlation between them. The temporal PSD_t of the raw EEG (Figure 3,A), the AP differences (B), and cospectrum (C) were calculated for the averages over channels. The frequency, f_m, at the maximum of the power, p_m, in the cospectrum was identified within the alpha range (7.5-12.5 Hz, Figure 3,C) rather than the theta range, owing to the predominance of alpha in the human scalp EEG.

Control values of f_m and p_m were first calculated without band pass filtering. Then an optimal value of $f_m = f_{opt}$ was found for the low pass filter in pass 1 (Figure 3, D) by fixing the high pass filter at 12 Hz and systematically stepping the low pass filter from 20 to 80 Hz in steps of 10 Hz. This gave a set of values for p_m in the form of a tuning curve. The frequency, f_{opt} (low), at the maximal value for p_m was chosen as the cut-off for the low pass filter. Next in pass 2 (Figure 3, E) the low pass filter was fixed at f_{opt} (low), and the high pass filter was increased in steps of 4 Hz from 4 Hz to 28 Hz. This gave a second tuning curve of values of p_m, from which the best high pass cut-off frequency, f_{opt} (high), was determined from the maximal p_m. This pass band was also use when maximal power shifted from the alpha range into the theta or delta ranges, because search outside the

alpha range for correlations between signed AP differences and the raw EEG failed to yield clusters of large jumps in AP differences.

The open source code developed and applied here for the Hilbert transform and the spatial and temporal filters is available for downloading in an anonymous file at the web site: http://sulcus.berkeley.edu.

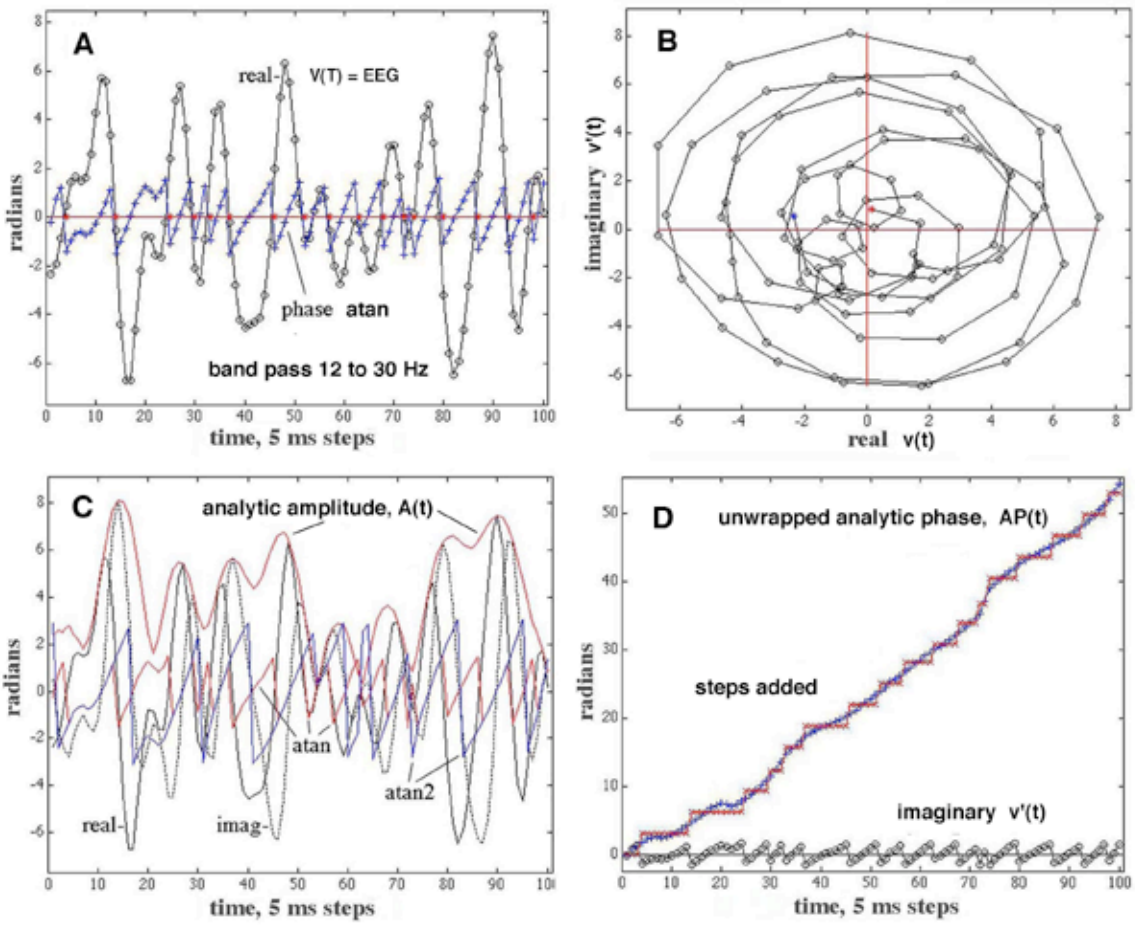

Figure 1. A. An example shows the EEG after it was band pass filtered (20-60 Hz). The sawtooth shows the analytic phase (AP) before unwrapping. The red asterixes show the estimated zero crossings. The open dots show the data points at 5 ms intervals. **B.** The polar plot shows that the two variables define a vector with its tip at each successive point on the loops. The vector rotates counterclockwise with time, giving the cumulative increase in AP with time. The length of the vector gives the analytic amplitude (AA, red envelope at left). The AP is the angle of the vector, which is computed from the arc tangent (red sawtooth, modulo π) and (blue sawtooth, modulo 2π). **C.** The real part of the EEG signal is shown by the solid black curve. The imaginary part (dotted black curve) approximates its time derivative. **D.** The phase after unwrapping shows an increase, for which the average slope is the frequency in radians/second, The unwrapped atan phase is shown on the abscissa. The steps in phase are added at the downward zero crossings of the sawtooth.

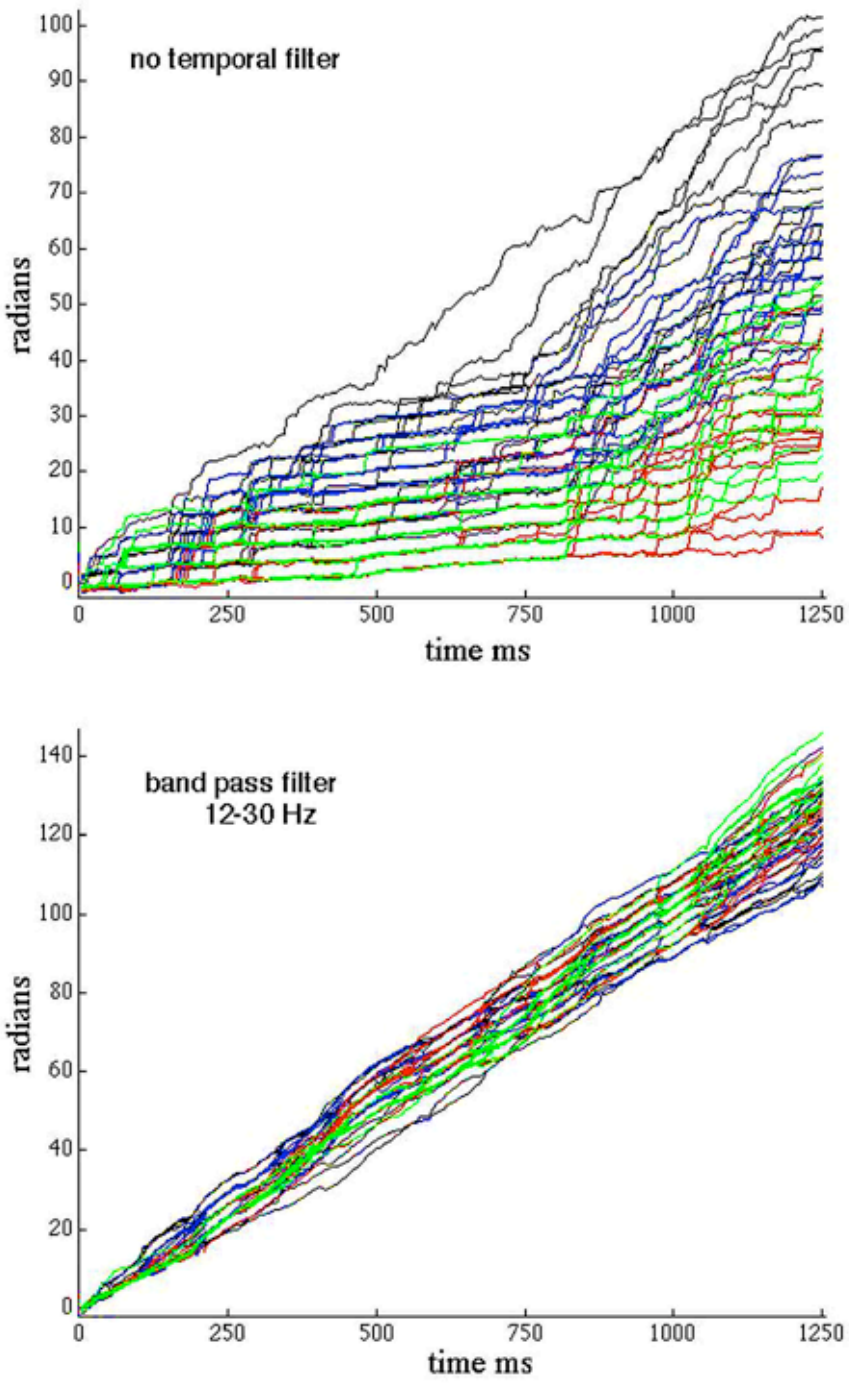

Figure 2. A. An example shows the analytic phase (AP) 64 EEG signals after unwrapping without band pass filtering. The colors show groupings of 16 adjacent channels. The staircase appearance manifests "phase slip", which is characteristic of broad-band noisy signals. **B.** The AP(t) from the same EEG signals are shown with band pass filtering to minimize phase slip. The task is to find and measure phase jumps that are physiological and not noise or computational artifacts.

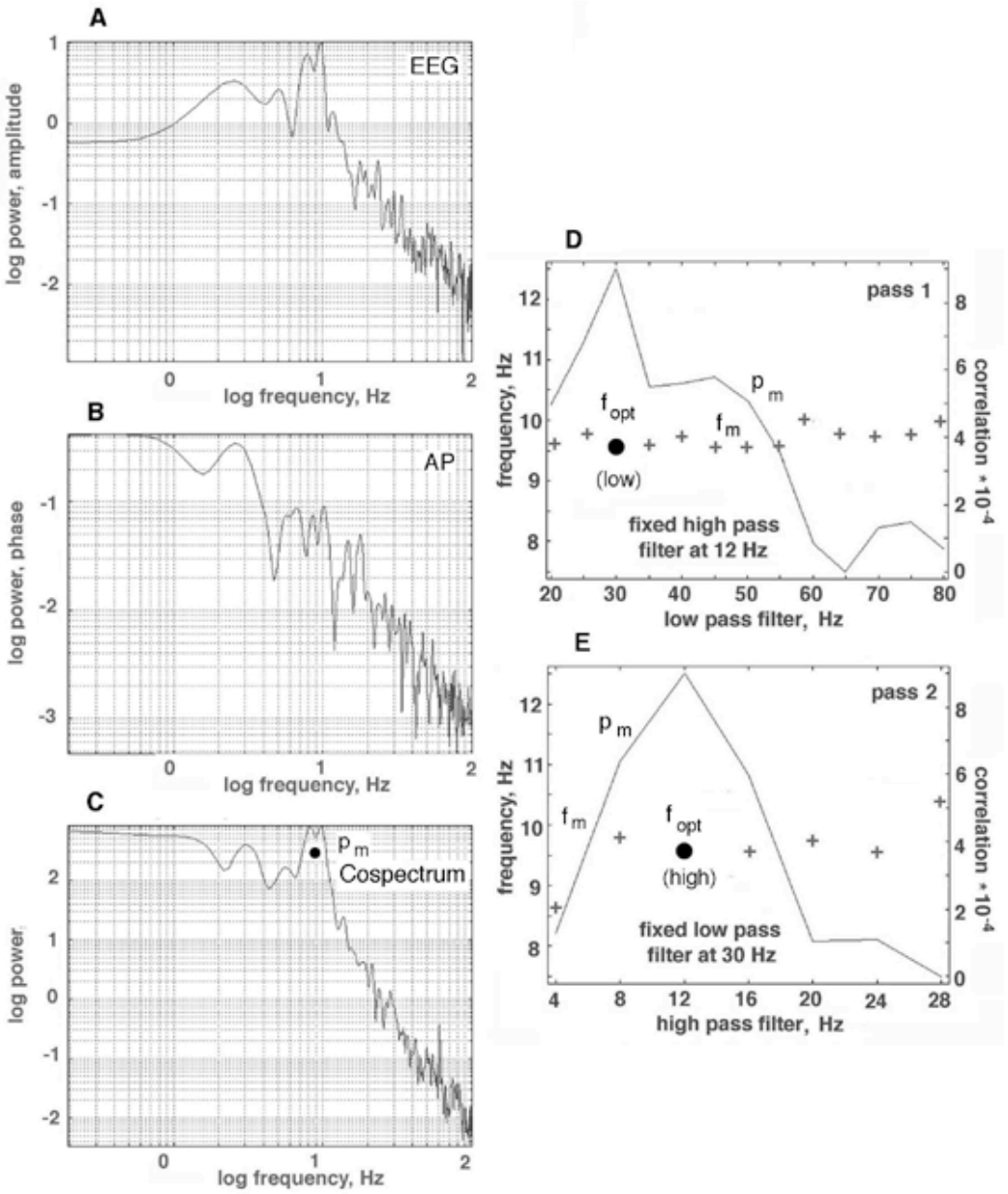

Figure 3. The technique for constructing tuning curves is illustrated. **A.** PSD_t of raw EEG from frontal cortex of a subject at rest with eyes closed **B.** PSD_t of signed temporal AP differences after filtering the EEG in a pass band of 12-30 Hz. **C.** Cospectrum of EEG and AP differences for the same pass band. **D**. The maximal value in the cospectrum of the cross-correlation (•) was sought in the alpha range (7.5 to 12.5 Hz) as a function of the pass band. Pass 1 was to fix the high pass filter at 12 Hz and vary the low pass filter setting. **E**. In pass 2 the low pass filter was fixed and the high pass filter setting was stepped. The alpha frequencies at which peaks were found for each filter setting are shown by crosses; the alpha frequency at the peak off the cospectrum is shown by f_{opt} (•).

Results

1. Application of the Hilbert transform to scalp EEG

To illustrate the recording arrangement a normal brain was obtained from a teaching collection. A montage was constructed of photographs taken from views perpendicular to the curved surface [Figure 4]. The radius of the brain was 7.5 cm, and the estimated thickness of the skull and scalp was 1.5 cm. The gyri appeared as light areas, and the outer aspects of the sulci appeared as dark curves, indicating the indentations in the wrinkled surface of the cortex. The circumference of the scalp of the nine subjects varied between 56 and 59 cm, giving an approximate radius of 9 cm for the head. The surface view of the cortex was up-scaled 20% to the area of the scalp. Superimposed rows of dots on the photographic montage indicate the length, spacing, and the three locations of the curvilinear array of recording electrodes. The EEG signals and EEG deliberately contaminated by EMG recorded from the linear scalp array were unremarkable (Figure 5).

Band pass filtering gave oscillations having fairly regularly spaced peaks and zero crossings. The AP appeared as a sawtooth time series (Figure 1, A). Unwrapping gave a ramp function (Figure 1, D) with minor irregularities and occasional dips (negative temporal AP differences). The instantaneous amplitudes of the EEG before and after the HIlbert transform at each digitizing step determined a point in the complex plane, which specified the tip of a vector extending from the origin at zero amplitude (Figure 1, B). The analytic amplitude (AA) was given by the length of the vector (the enveloping red curve in C) from equation (4). The analytic phase (AP) was given by the angle between the vector and the real axis in B, which was evaluated with equation (5). The vector rotated counterclockwise with successive time points, thereby tracing a loop with each cycle. Usually the loops went around the origin and enclosed it, but, as shown in this example, smaller loops might fail to circumscribe it. The shortfall in the loop caused brief periods of negative AP differences (Figure 1, B). In (C) the black solid curve showed the real part of the Hilbert transform, which was identical to the EEG. The dotted black curve showed the imaginary part, which approximated the time derivative of the EEG. The two sawtooth functions in C compared the AP values derived using the arc tangent modulo π (atan) and the arc tangent modulo 2π (atan2). The atan function was found to have fewer outlying phase values than the atan2 function, so it was used routinely. The sizes of the jumps varied as the slope of the unwrapped AP fluctuated, most markedly when the AA was low.

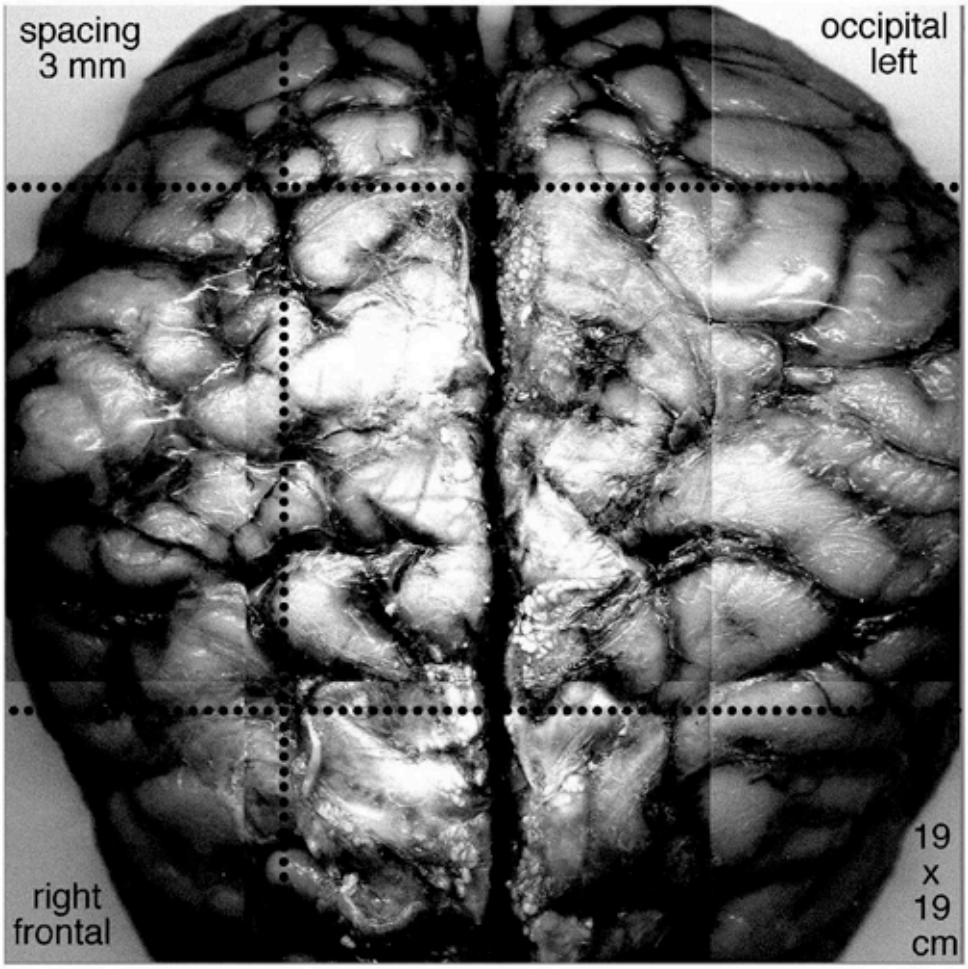

Figure 4. A montage of photographs shows the surface of a human brain specimen from a teaching collection. The light areas are gyri, and the dark lines are sulci. The scale has been expanded 20% from the radius of the brain, 7.5 cm, to the radius of the scalp, 9.0 cm to visualize the projection of the gyri onto the scalp. The rows of dots show the three locations of the 64x1 array of scalp electrodes: frontal, paracentral and occipital. Adapted from Freeman et al., 2003.

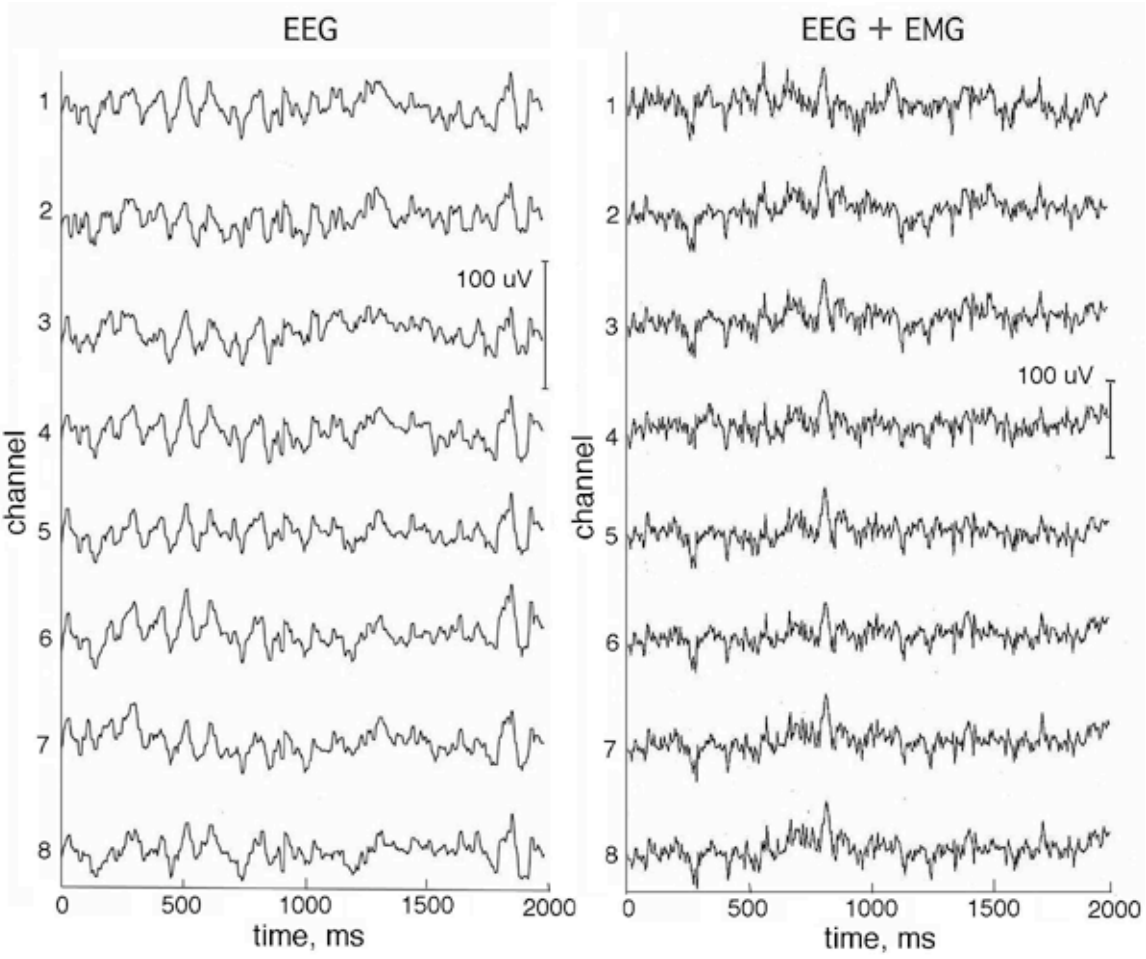

Figure 5. A contiguous subset of 8 out of 64 EEG traces from the paracentral scalp of an alert subject with eyes closed, at rest (left) and while inducing a modest level of EMG (right) by tensing the scalp muscles. Reference: ipsilateral mastoid.

2. Derivation of PSD and use of band pass filters

The temporal power spectral densities (PSD_t) of the EEG and AP (Figure 3) both showed linear decrease in log power with increasing log frequency, the "1/f" form but with local spectral peaks in varying ranges (Freeman et al., 2003). The Hilbert transform increased relative power in the AA at low frequencies and increased it at high frequencies. The amplitude histograms of the EEG were well approximated by the Gaussian function (Freeman, 1975). Histograms of the AA resembled the F-distribution, as expected to describe variances and covariances, extending from zero to a peak near 1 standard deviation (SD) and a long tail with high values. The effects of the band pass filters on the distributions of sequential AP differences were examined in two ways. First, the center frequency of the pass band was fixed at 40 Hz, and the pass band was changed in steps of ±5 Hz from ±2.5 Hz to ±12.5 Hz for comparison with high pass filtering at 2 Hz (Figure 6). The distributions were leptokurtic with high central peaks. The long tails ranged slightly beyond $\pm\pi$ for the atan function especially for the unfiltered EEG. For comparison, the step size of 5 ms would give an AP difference of $\pm\pi/2$ radians at 52 Hz and ±0.8 radians at 14 Hz. The filtered data showed progressive diminution of the SD of the distributions with decreasing band width (Figure 7, left frame). The "normal" SD for a Gaussian density distribution fitted to the center peak (omitting the tails as outliers) averaged 0.6 of the actual SD. The mean AP difference was relatively independent of band width. Second, the band width was fixed at ±5 Hz, and the center frequency was stepped at 10 Hz intervals. The mean value of sequential AP differences co-varied with band width, but the SD did not (right frame).

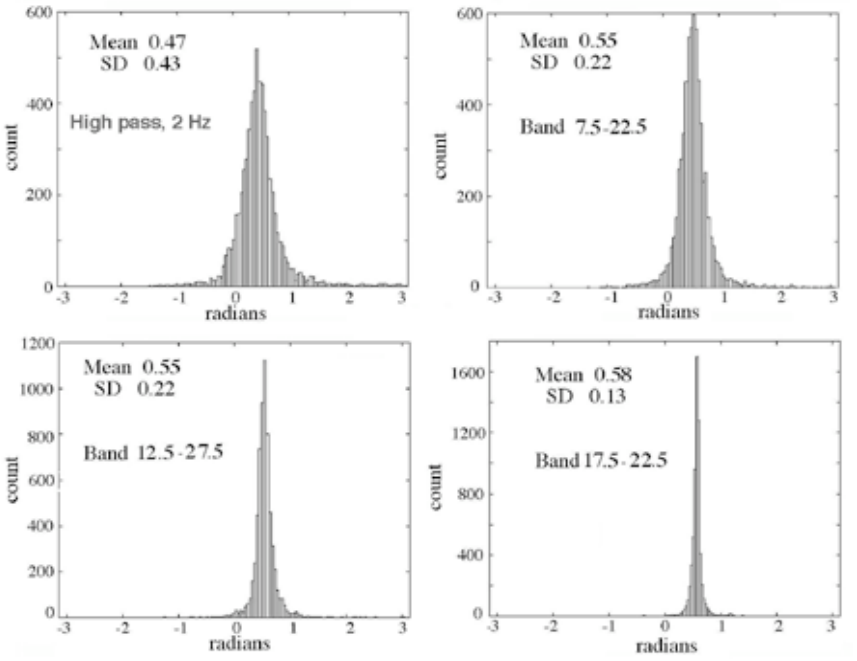

Figure 6. The distributions of sequential AP differences after temporal filtering of the EEG before applying the Hilbert transform are shown for band widths that all had the same center frequency of 40 Hz.

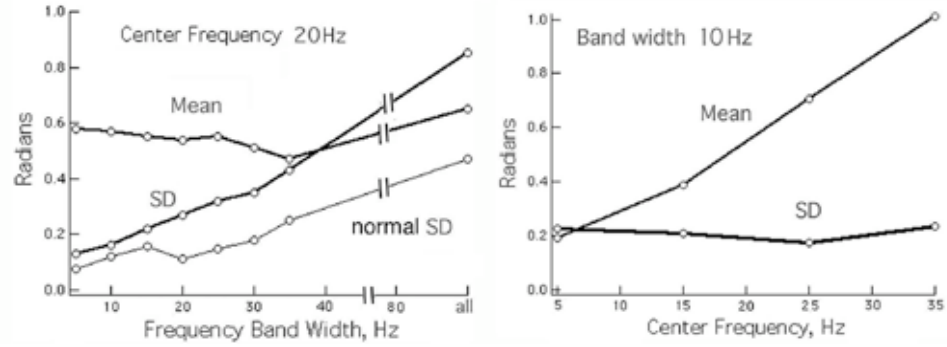

Figure 7. The relations are shown between the mean and SD of the sequential AP differences and variation in the band with or center frequency. The "normal" SD was derived by fitting a Gaussian curve to the center peak, omitting the tails. **Left:** The center frequency was fixed, and the band width was varied. **Right:** The band width was fixed, and the center frequency was varied.

3. Spatial clustering of temporal phase slip across channels

The relatively small number of large sequential AP differences tended to occur in spatiotemporal clusters on multiple adjacent channels within 2 to 4 samples (10 to 20 ms at the 5 ms digitizing interval). Figure 8 shows a typical example of the sequential differences (the numerical rates of change used to approximate the time derivatives, and to estimate the instantaneous frequencies in radians/s of the AP by dividing by the digitizing step of 2 ms) for 16 signals from adjacent electrodes. The maximal differences were either positive and negative in the same time frame, sometimes appearing biphasic (steps 70-74, channels 56-64 in Figure 8) which was not unusual for the Hilbert transform, especially when the segment length was not a power of 2. The direction of change in AP was less important than the timing, so the absolute lAPl differences were plotted for the entire array as time functions in 2-D, after subtracting the global means (Figure 6). An example from the frontal area of a subject with eyes closed and high alpha activity shows that the lAPl jumps were often synchronous across part or all of the array (Figure 9). The locations in time and space of the synchronized AP jumps varied depending on the width of the pass band, and on the presence or absence of alpha or theta activity in the EEG, here with prominent alpha. Figure 10 shows the spatiotemporal clusters from another subject, also recorded over the frontal area with eyes closed but with no alpha activity and minimal theta. The times at which spatiotemporal clusters were revealed tended to vary with the center frequency of the narrow pass band. These findings held also for the paracentral and occipital areas in the presence and absence of alpha or theta or both.

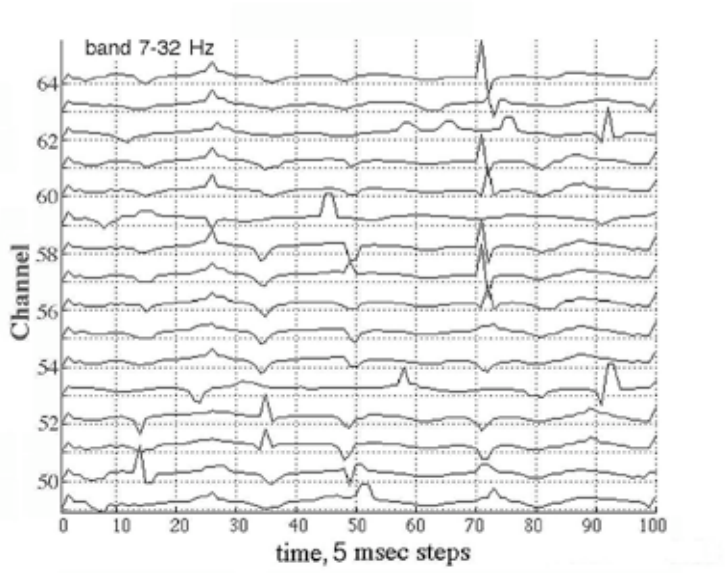

Figure 8. A representative set of EEG from 16 of 64 consecutive channels shows sequential differences, AP(t) - AP(t-1), at the digitizing step of 5 ms after filtering in the pass band of 12-30 Hz. The issue is to distinguish the jumps due to cortical dynamics from those due to phase slip from noise, nonlinearities, and numerical artifacts.

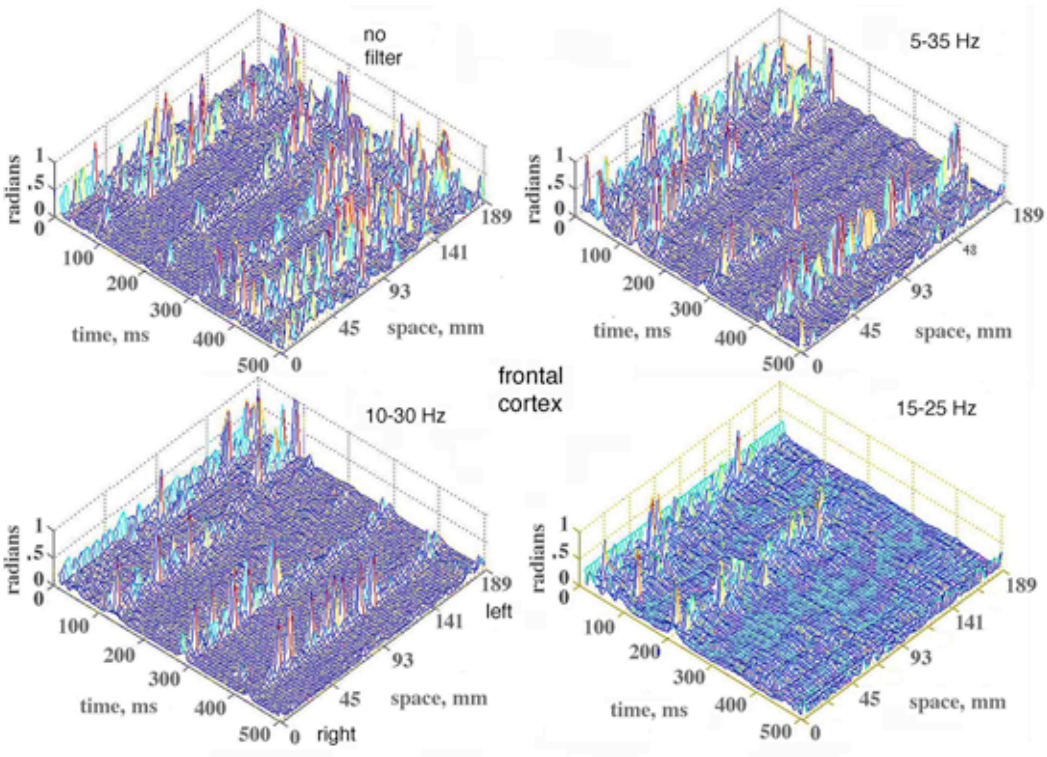

Figure 9. The absolute values of temporal AP differences, lAPl, are shown for 64 channels (right abscissa) of the 18.9 cm curvilinear array in a 500 ms epoch (left abscissa). The differences are shown for 3 pass band widths with the center frequency fixed at 20 Hz for comparison with the unfiltered EEG For optimal display the lAPl values >1 radian were clipped at 1 radian. Frontal area, eyes closed, channels numbered right to left across the midline, vertex reference.

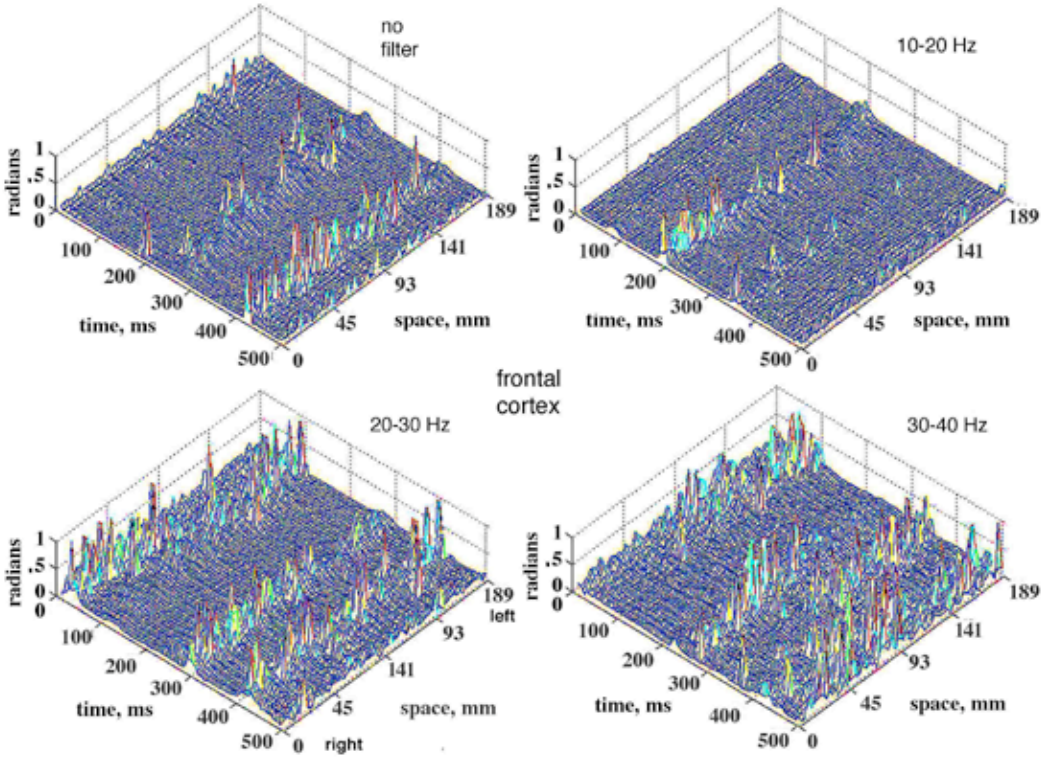

Figure 10. Absolute temporal lAPl differences are shown for 64 channels in the 18.9 cm curvilinear array. They were computed in a 500 ms segment after band pass filtering the 64 EEG with 3 center frequencies. The band width was fixed at 10 Hz for comparison of lAPl differences with no filler. Frontal area, eyes closed, 0 to 64 right to left across the midline forehead, vertex reference.

4. Using AA differences to enhance visualization of AP differences.

Correlation of the AA(t) and AP(t) showed that wide excursions in the time derivative of the AP in either direction often accompanied substantial decreases in AA on the same channels. The spatial ensemble average of the fluctuations in AA over the 64 channels in a 1.25 s epoch are shown by the blue curve Figure 11,A. The standard deviation (SD) of the spatial AA differences at each time step (red curve) was relatively constant despite the wide fluctuations in the mean on each channel. The vertical bars were drawn where the average AA fell below an arbitrary threshold of 1.75. The absolute values of AP were taken after subtraction of the mean corresponding to the frequency. The average absolute lAPl after demeaning (Figure 11,B, blue curve) and its SD over the 64 channels (red curve) co-varied closely. The peak lAPl values tended to occur at the minima of AA, as shown by the vertical bars extended from frame A. The distribution of the 250 pairs of AA and lAPl in a representative EEG segment lasting 1.25 s (Figure 12, A) confirmed the inverse relation.

The distribution of the average values of lAPl is plotted as a function of average values of AA in Figure 13, A, showing the tendency for low AA to be accompanied by high lAPl. The distribution of the signed AP differences from the 64 channels (Figure 12, B) prior to de-meaning shows the mean frequency as the positive offset. Most of the AP differences are positive. the small number of negative and unusually high positive values were paired with low values of AA, although the majority of minima in the AA were not accompanied by concomitant extremata in the AP differences.

The effect of weighting the lAPl differences by W is shown in Figure 13. Without weighting the synchronized changes in differences from the mean were both upward and downward though always positive. With weighting the dips were reversed to upward deflections, and the plateaus between jumps were smoothed.

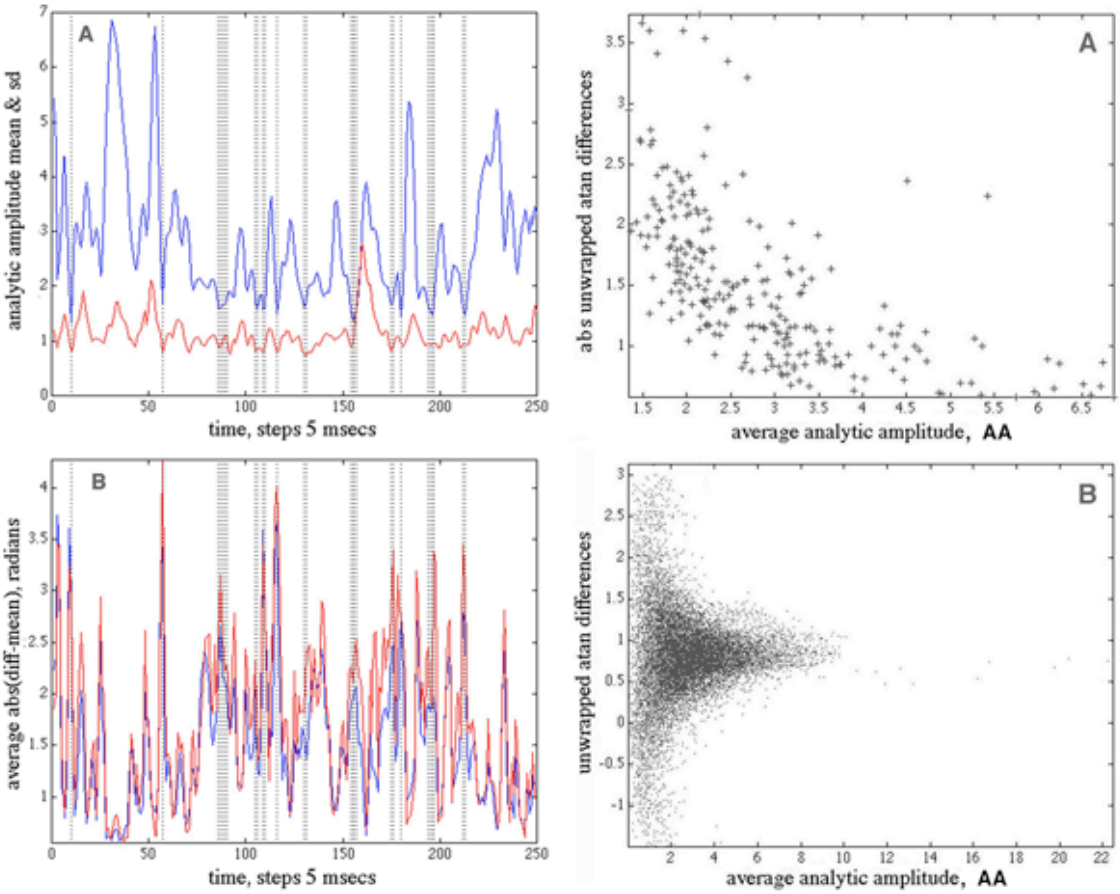

Figure 11. (left) A. The average (blue curve) and SD (red curve) were calculated for the AA(t) values from the 64 EEG in a 1.25 s epoch. The vertical bars indicate times at which the average AA fell below an arbitrary threshold of 1.75. N = 250.

B. The average (blue curve) and SD (red curve) of the absolute lAPl sequential differences showed peaks tending to occur at times when the average AA approached a minimum. N = 16,000. Paracentral area, eyes closed, EEG pass band 15-55 Hz.

Figure 12. (right) The relations among AA, AP and W were examined graphically. **A.** The absolute temporal differences lAP(t) - AP(t-1)l were averaged over the 64 channels in a segment 1.25 s long sampled at 2 ms intervals (N = 250) and plotted against the AA(t) averaged across channels at the same times. An inverse relation was found between AA and lAPl.

B. Signed AP temporal differences were plotted against AA amplitudes for all 64 channels and time points (N = 16,000), showing the preponderance of large deviations in signed AP from the mean with low values of AA. Paracentral area, eyes closed, EEG pass band 15-55 Hz.

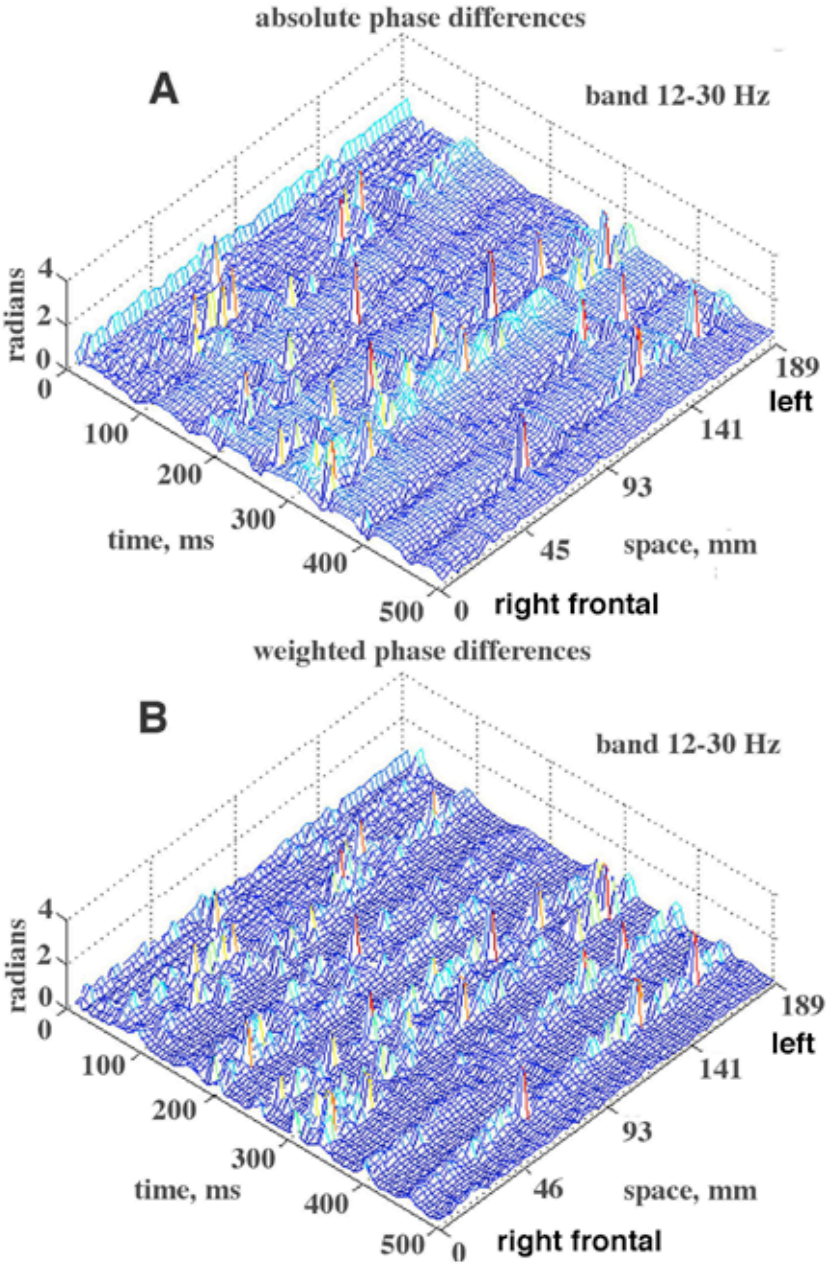

Figure 13. A. The spatiotemporal clustering of absolute lAPl differences on 64 channels in a 5 s epoch showed both dips and peaks tending to synchronize over the whole array, but with interhemispheric offsets. **B.** The absolute lAPl differences weighted by equation (6) were all upward, with some sharpening of clustering. Frontal area, channel numbering right to left, eyes closed, pass band 12-30 Hz. For the PSD_t see Figure 3,A.

5. Using tuning curves to minimize effects of phase slip

Figure 3 showed the spectrum of the autocorrelation of the EEG in frame A and the spectrum of the autocorrelation of the signed AP differences in frame B. The peak in the alpha range of the cospectrum of the cross-correlation averaged over all 64 channels (C) was found to be maximal with the pass band prior to the Hilbert transform set at f_{opt} (low) = 12 (D) and f_{opt} (high) = 30 Hz (E). The average value and SD for the alpha frequency at the peaks of correlation (indicated by •) were 8.93 ± .67 Hz, with no significant differences between occipital, paracentral and frontal areas. This pass band, 12-30 Hz, for optimizing the clusters of AP changes (CAP) synchronized with alpha was found in 8/9 subjects. The synchrony of the CAP jumps was again clarified by weighting the absolute time differences of the AP across the array with equation (6). In an example (Figure 14) from the paracentral area a subject at rest with eyes closed (A) was asked to open the eyes (B). The peak EEG frequency in the autospectrum and cospectrum shifted into the theta range. The CAP in this case were found over the frontal area and not over the parietal area, and the spatial distribution of CAP persisted at the lower recurrence rate. In another example (Figure 15) from the paracentral area the subject at rest with eyes closed was asked to tense the scalp muscles. There was no alpha peak in the PSD_t of the EEG or the cospectrum (left frame). With onset of EMG a weak alpha peak emerged in the cospectrum, and the stripes of CAP persisted in the parietal area. Despite the increase in power in the beta and gamma ranges contributed by the EMG, as documented in detail in a companion report (Freeman et al., 2003), the synchronized clusters of CAP were clearly visible (B) over the posterior third of the array.

These examples illustrated the way in which the curvilinear array could be used to estimate phase velocity. The variation of the AP jumps from the mean time of occurrence in the CAP stripes in some instances was within the 5 ms digitizing step over the array length of 18.9 cm independently of the orientation of the array. Whatever the delay over the array, the phase velocity would have had to exceed 40 m/s in the direction parallel to the array, and 20 m/s in directions ±60° from the array. For lesser velocities the peaks in the CAP would have lain diagonal to the right abscissa in the mesh plot, as in fact was occasionally noted in short segments.

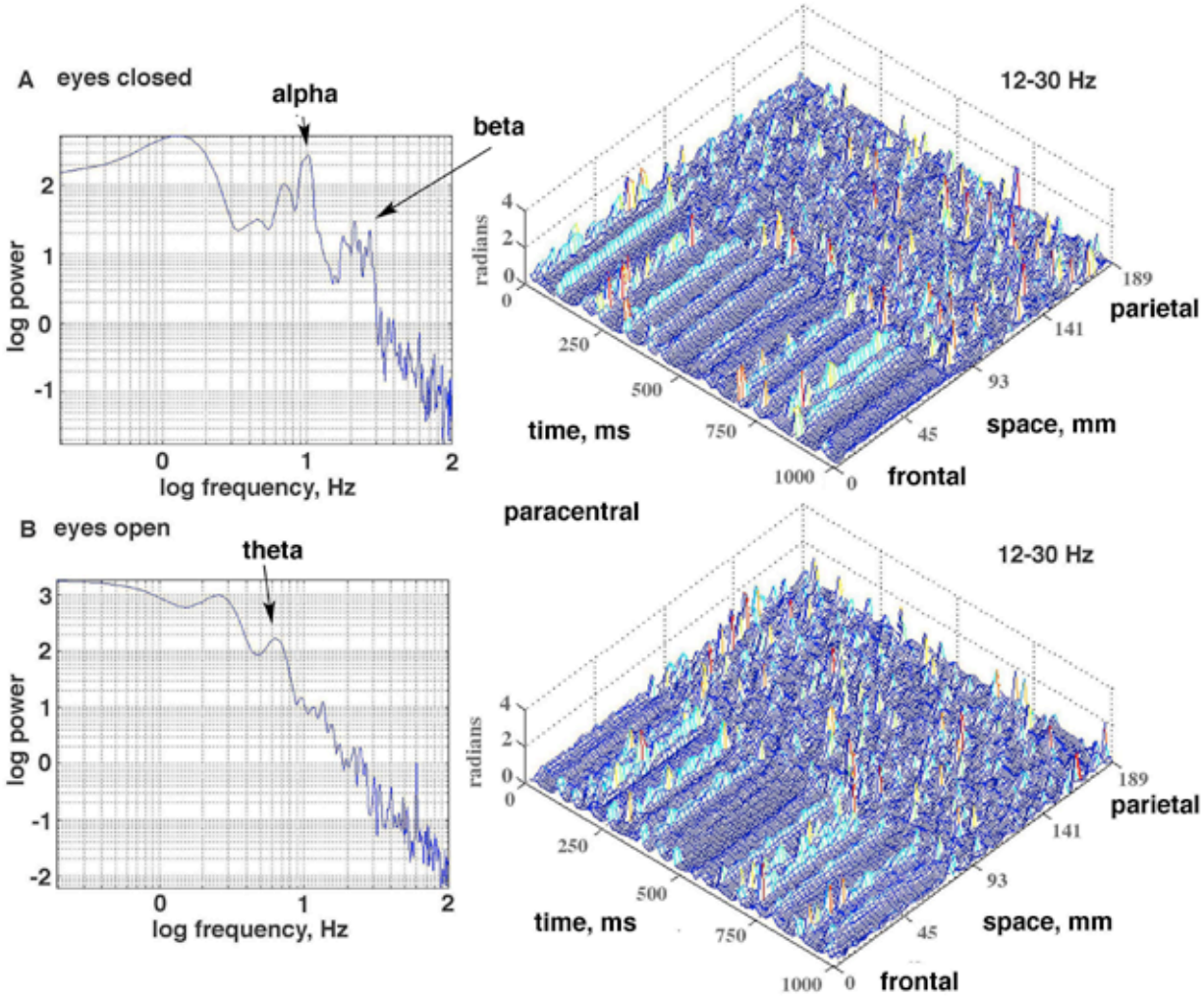

Figure 14. A. With eyes closed the weighted lAPl differences were spatially correlated in stripes that repeated at intervals in the alpha range (cospectrum in left frame) across the right paracentral area anteriorly (channels 1-30) but not posteriorly (right frame). **B.** With eyes open the spatial correlation of the clustered AP differences (CAP) persisted but repeated at a mean frequency in the theta range in accordance with the cospectrum (left). The optimal correlation was sought in the alpha range for both conditions. Epoch duration: 1 s.

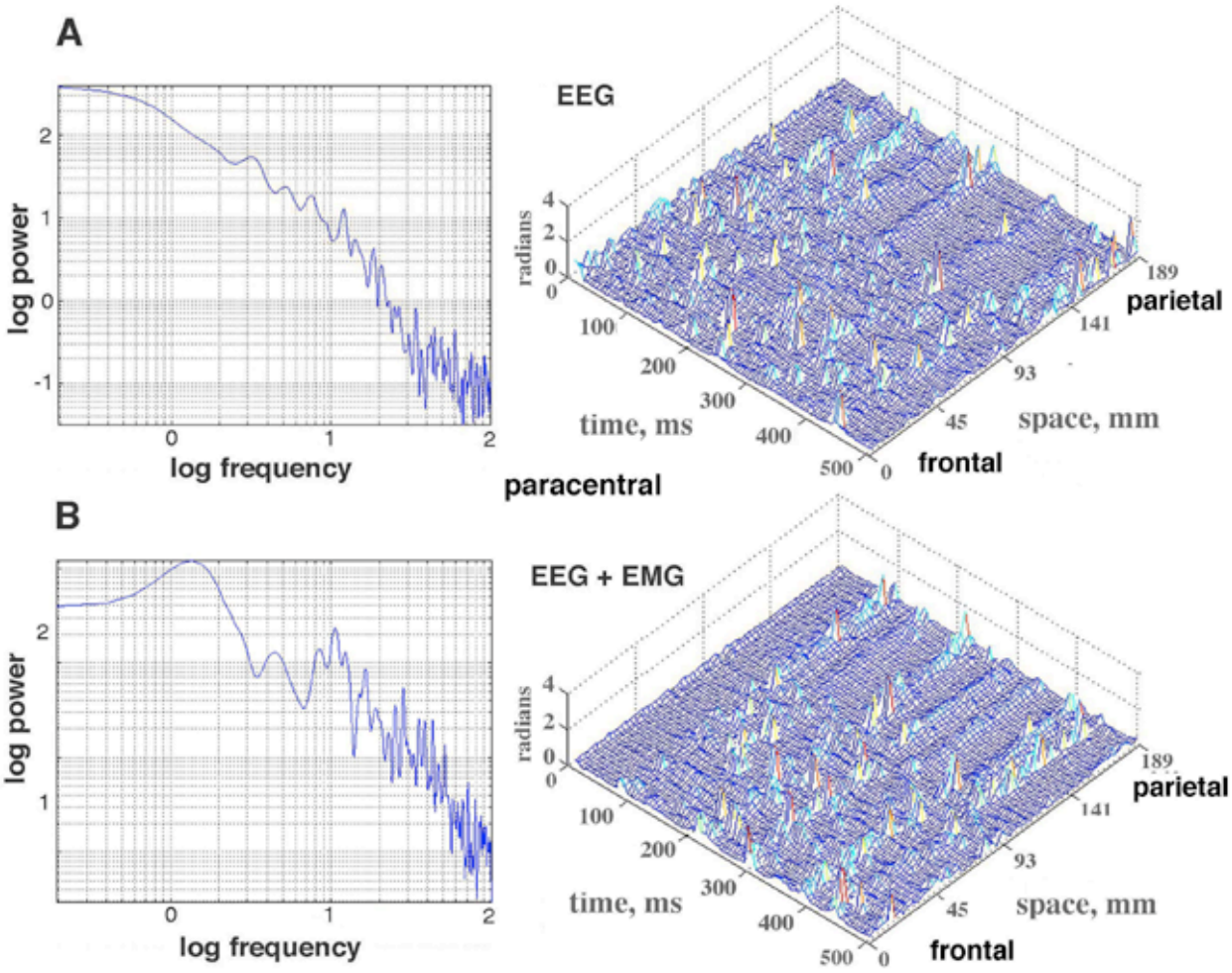

Figure 15. A. A subject at rest with eyes closed gave spatially ordered peaks in CAP in the paracentral area posteriorly (right frame) but with no alpha in the EEG or alpha peak in the cospectrum (left frame). **B.** With deliberate induction of EMG the amplitude of the signals increased across the entire spectrum (right frame). CAP persisted in the same parietal area (right frame). Epoch duration: .5 s.

6. Other manipulations of the AP differences prior to display

The effects on the CAP of three types of randomization were examined (Figure 16). A data set was processed from the occipital cortex of a subject at rest with eyes closed that showed CAP stripes bilaterally (A) with temporal filtering at 12-30 Hz. Randomization of the channels (B) by reordering them with a table of random numbers introduced noise without significant loss of the CAP. Surrogate data were generated by taking the FFT of the filtered EEG on each channel, randomizing the phase values, and taking the inverse FFT, thereby keeping the power and second order statistics intact. This procedure (C) diminished but did not abolish the CAP. Shuffling was done by using a table of random numbers to select at random a time point in each EEG and translating the later segment to precede the earlier segment. This re-ordering (D) of the sequences on the channels destroyed the CAP.

Spatial filtering of the EEG applied before temporal filtering further clarified the CAP. The choice of low pass filter setting was based on the 1-D spatial PSD_x of the 64 raw EEG amplitudes, averaged over 1,000 time points (500 steps) (Freeman et al., 2003). Examples of PSD_x from four subjects are shown in Figure 17,A from the frontal cortex with no temporal filtering. Typically the rate of decrease in log power with log frequency did not conform to 1/f for scalp EEG as it did for intracranial EEG (Freeman et al., 2000), and small peaks figured persistently in the range of 0.1 to 0.5 c/cm. For comparison with the anatomy, the photographic montage (Figure 4) was digitized at a grain of 1 mm, and the two-dimensional FFT was used to calculate the spatial spectrum of the image of the cortical surface [Figure 17, B]. The basic form of the spatial spectrum of the montage was $1/f^{\alpha}$, where α = -1.7, with a broad peak in the range of 0.1 to 0.5 c/cm, corresponding to the typical length (3-5 cm) and width (1 cm) of human gyri. A low pass spatial filter was set at 1.05 c/cm to smooth variations near the Nyquist frequency (1.67 c/cm), at 0.40 c/cm near the width of gyri, and at 0.167 c/cm near the length of gyri.

The effect of spatial filtering is shown by the example in Figure 18. A control with no spatial filter is shown from the occipital cortex of another subject (A). The two hemispheres did not show synchrony. The array length of 18.9 cm and spacing of .3 cm set a low frequency bound of .053 c/cm and an upper Nyquist bound of 1.67 c/cm. A low pass filter was applied to the EEG data before temporal band pass filtering with a set point at 1.05 c/cm (B), then at 0.4 c/cm (C) and 0.167 c/cm (D). The clarity of the CAP was progressively improved. The effect of a high pass filter on the CAP from the frontal cortex (Figure 4, lower row of dots).of a subject at rest with eyes closed is shown in Figure 19. Compared with the control in (A) the filter set at 0.1 c/cm virtually abolished the CAP from the mesh plot (C). Re-referencing by subtracting the spatial ensemble average (B) obscured the CAP and at the same time diminished the alpha peak in temporal spectra from the frontal area (Freeman et al., 2003). This decrease did not occur with re-referencing in spectra and mesh plots from the paracentral and occipital areas. Shifting the temporal pass band from 12-30 Hz to 20-40 Hz (D) or yet higher spectral ranges preserved the CAP stripes but shifted them to new time locations. This effect introduced a new dimension to the study of CAP, which was too complex to be explored in this introductory study.

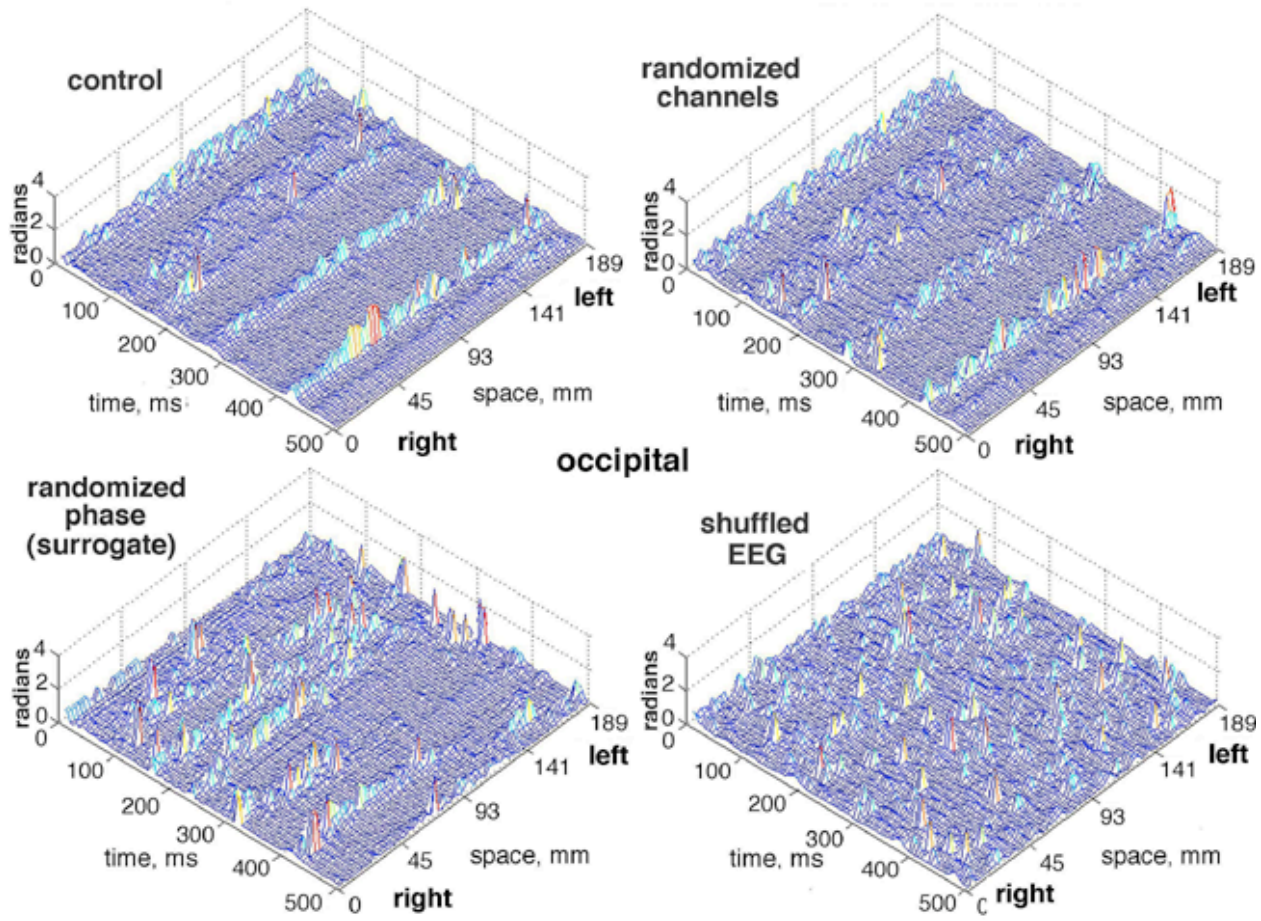

Figure 16. Three types of statistical control are illustrated. **A.** The control mesh shows CAP stripes extending across occipital areas bilaterally with the pass band set at 12-30 Hz. **B.** The channel order was randomized. **C.** The EEG signals were transformed by the FFT, the phase values were randomized, and the inverse FFT was taken to generate the surrogate signals. **D.** The EEG were shuffled by segmenting the signal on each channel at a time point chosen at random and translating the latter portion from after the point to before.

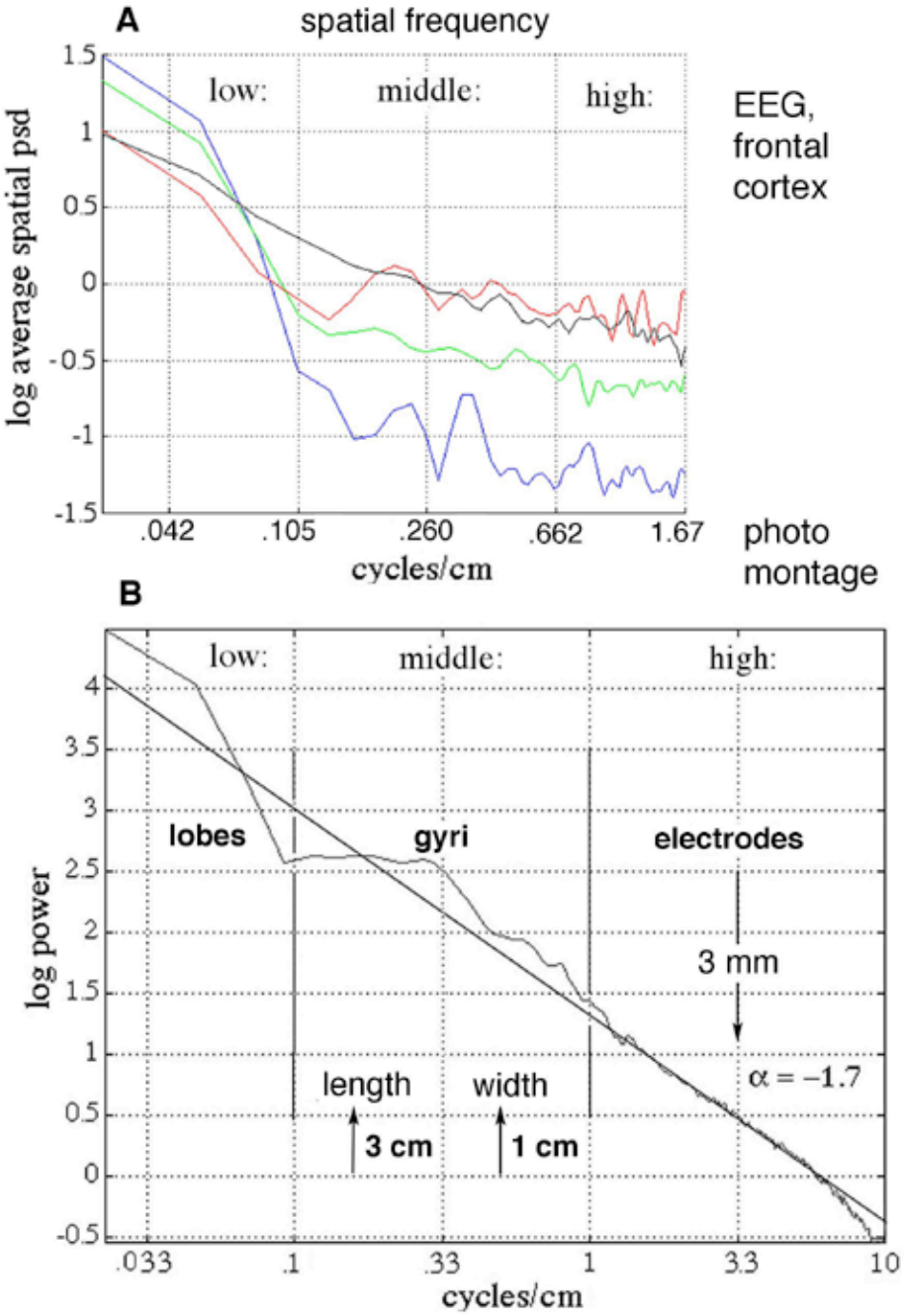

Figure 17. A. Examples are shown of the spatial spectra (PSD_x) from the frontal cortex of four subjects at rest with eyes closed. **B.** The 2-dimensional FFT was taken of the photograph in Figure 4 digitized at 1 mm steps to get the spatial power spectral density, PSD_x. The central peak corresponded to the typical length (3 cm) and width (1 cm) of gyri, and to peaks in the PSD_x of the EEGs. The spectral form was $1/f^{\alpha}$, where α = -1.7 Adapted from Freeman et al., 2003.

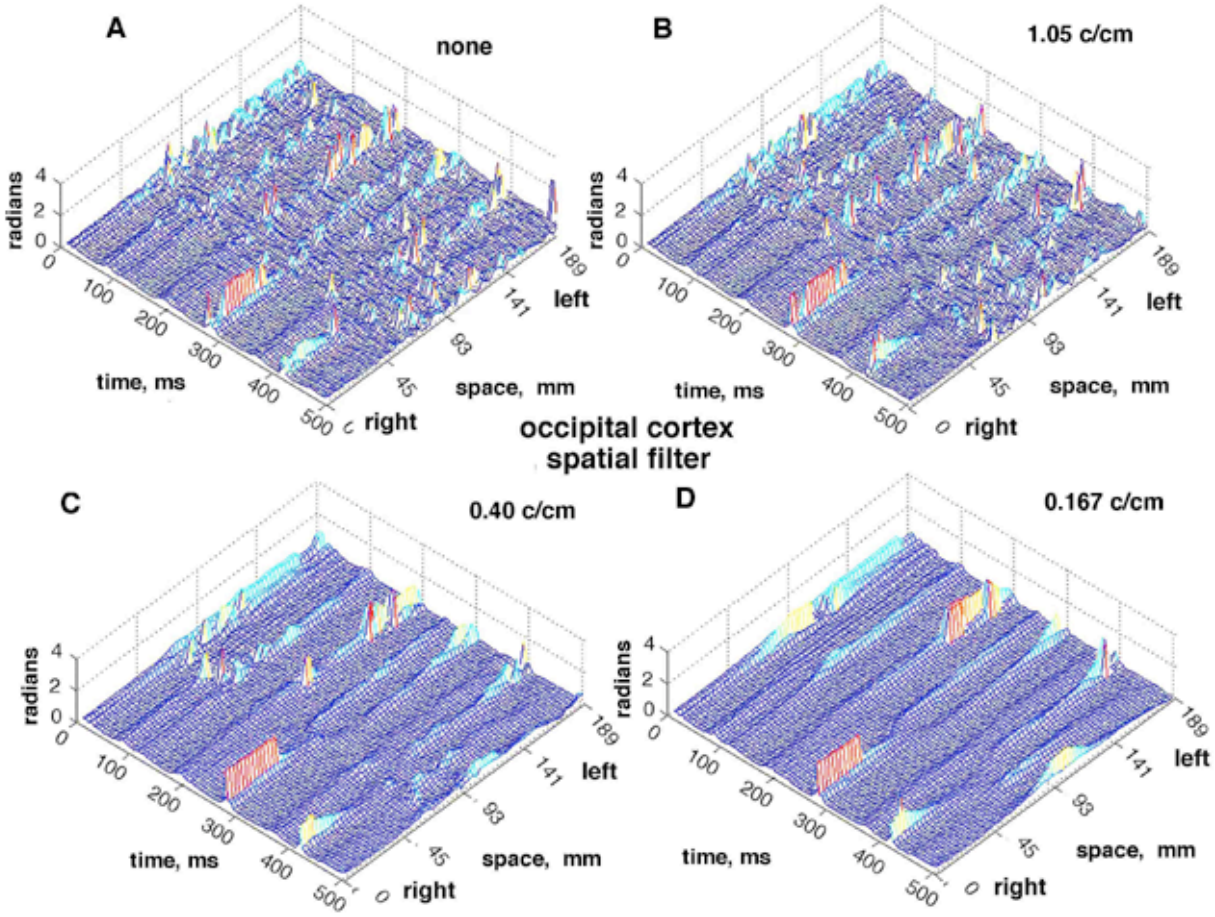

Figure 18. The effects on the CAP are illustrated of applying a low pass spatial filter to the 64 EEG signals after global de-meaning and prior to temporal band pass filtering. **A.** No filter. **B.** 1.05 c/cm (wave number = 6.6 radians/cm, wave length = 9.5 mm). **C.** Filter at 0.4 c/cm (wave length = 25 mm). **D.** Filter at 0.167 c/cm (wave length = 60 mm).

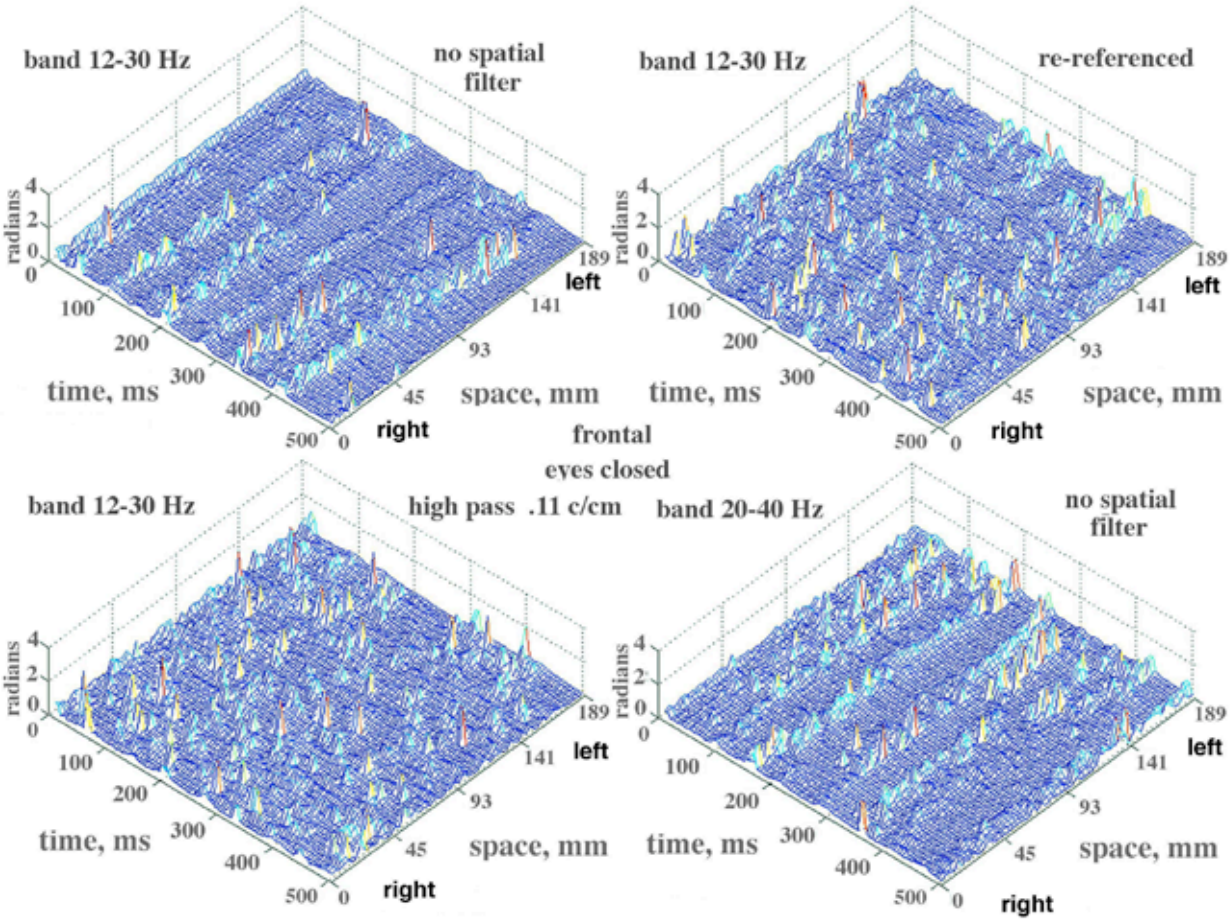

Figure 19. Three types of data manipulation are illustrated. **A.** The EEG of a subject at rest with eyes closed yielded CAP in the frontal area bilaterally with some dissociation between locations. The optimized pass band was 12-30 Hz. **B.** The CAP disappeared on re-referencing by subtraction of the spatial ensemble average. **C.** A high pass spatial filter set at .042 c/cm (wave length exceeding the length of the array) also suppressed the CAP. **D.** Shifting the pass band to 20-40 Hz retained the CAP but shifted the stripes to different times and locations. Epoch duration: .5 s.

Discussion

1. Advantages and limitations of the Hilbert transform

The rationale for adapting the Hilbert transform to analysis of scalp EEG was based on the hypothesis that abrupt changes in cortical states occur stepwise at rates in the delta, theta and alpha ranges (Freeman and Rogers, 2000). Such changes had been seen in EEG recorded in animals intracranially (Freeman and Barrie, 2000; Freeman, 2003a). From estimates of their spatial distributions in sensory cortices the stepwise changes appeared to be synchronized over distances that might make it possible to detect them in scalp EEG, if indeed these or similar abrupt changes occur in human cortex. The changes in animals had the form of synchronized modulations of amplitude, frequency and phase of the ongoing oscillations of EEG recorded from multiple locations. Owing to its high temporal resolution (equal to the digitizing rate) the Hilbert transform was deemed to be more likely than Fourier-based procedures to enable precise temporal localization of the abrupt changes, accompanied by precise spatial localization afforded by the high-density array of electrodes.

The main difficulty in using the Hilbert transform arises from the intrinsic discontinuities in the AP function that necessitate unwrapping. As seen in Figure 3, A the amplitude and rate of change of an EEG signal can be represented by a vector, for which the change with time is in its length and its rotation about the origin of the complex plane, usually counterclockwise. The procedure allows the display of the EEG amplitude and phase as independent variables. The rotation gives a ramp-like increase in phase with time, but with breaks when the vector crosses the imaginary axis (re-setting the phase by $-\pi$) or the negative real axis (re-setting the phase by -2π). The difficulty of the correction by unwrapping to give a continuous ramp lies in predicting the size of the phase increment across the break. The additive step in AP is easy to predict when signals are periodic, but it can be very difficult with the noisy, aperiodic signals of EEG (Pikovsky, Rosenblum and Kurths, 2001), especially when the EEG dithers above or below zero without crossing. In the case of unfiltered EEG having the 1/f form of PSD the AP has the appearance of a random walk or a Markov process known as "phase slip". The difficulty becomes most obvious in displays of the signals from multiple channels, which as time series are highly coherent (Figure 5), but the AP(t) differences diverge in staircase form with jumps predominantly near π radians (Figure 2).

On the one hand, in both theory and practice (Freeman and Rogers, 2000) an increment in AP(t) signifying a physiological change in cortical state can be negative or positive (backward or excess forward rotation) or so small as to be indistinguishable from the average increment. Especially if the state change occurs as the vector crosses an axis of the complex plane, it may be missed altogether. On the other hand, there are several ways in which unusual increments can appear in EEG from arrays of electrodes, due to thermal noise or movement artifacts on one or more channels. The beating of two periodic components with nearly the same frequency can give a phase jump when the sum of amplitudes goes through zero. A high frequency component riding on a low frequency component can cause a failure of an expected zero crossing. This may be exemplified in Figure 1, B, where loops of the trajectory of the vector sometimes fail to enclose the origin, and the AP differences are briefly negative (Figure 12,B). If the noise or the mixed frequency components were to occur at the reference electrode with referential recording, then increments of unusual size would appear on most or all of the channels. Hence the Hilbert transform can miss state changes, and it can generate false reports of state changes.

One recourse is to narrow the pass band of the temporal filter so as to reduce phase slip. Studies by Le Van Quyen et al. (2001) and Quiroga et al. (2002) have shown that measurements of phase by the FFT and the Hilbert transform with very narrow pass bands give nearly equal values, showing their equivalence under this constraint. However, the temporal resolution offered by the Hilbert transform is compromised by narrow band filtering, and the opportunity to track nonlinear frequency modulation in the form of phase modulation, giving temporal coherence to chaotic time series, is lost. Therefore, some band pass filtering is necessary, but not to the point of significant impairment in temporal resolution.

2. Determination of optimal time windows and spectral pass bands

The further hypothesis emerged from animal studies that there are two main classes of EEG oscillations that are required for cortical states and state changes: low gating frequencies in the delta and theta ranges, and high carrier frequencies in the beta and gamma ranges. Sensory cortices in rabbits and cats with arrays of electrodes surgically implanted subdurally have revealed wave packets as brief epochs of spatially coherent oscillation in the beta and gamma ranges. The wave form of the shared oscillation has been found to have spatial patterns of amplitude modulation (AM). The AM patterns served to classify EEG epochs with respect to conditioned stimuli that the animals had learned to discriminate after classical or operant conditioning (Freeman and Viana Di Prisco, 1986; Ohl, Scheich and Freeman, 2001). The wave packets also had spatial phase modulation (PM) of the carrier wave in the form of a cone, for which the location and sign (maximal lead or lag) varied at random across successive wave packets without relation to the conditioned stimuli. The spatial phase gradient in radians/mm (the slope of the PM cone), when it was converted to m/s with the center frequency of the carrier wave, conformed to the range of conduction velocities of intracortical axons running parallel to the pial surface (see references in Freeman and Baird, 1987; Freeman and Barrie 2000; Freeman, 2002). The time period required for a phase change was estimated to range from 3-7 ms, and the durations of wave packets were estimated to range from 76-101 ms. The recurrence rate averaged 4.01±1.53 Hz, so the time interval between wave packets ranged from 80-324 ms (Freeman, 2003a).

These numerical estimates supported the predictions in the time domain that jumps in phase of unusual size with the Hilbert transform would be synchronous in local areas of cortex within 3-7 ms, and that the distribution of increments in the same state change would include both directions (forward or backward, lead or lag) and at some locations no detectable AP difference (Freeman and Rogers, 2002). The estimates provided an essential guideline for designing synchronization indices by applying an 80 ms moving window to the data for de-meaning and calculation of Shannon entropy. In the spatial domain, most wave packets in animal studies were 1 to 3 cm in diameter with a mode of 1.5 cm, so that if they occurred in that size range in human cortex, they would be detectable at the scalp in signals from only 3 to 9 contiguous electrodes with 3 mm spacing. In a preceding report on the spatial and temporal spectra of EEG (Freeman, Holmes, Burke and Vanhatalo, 2003), the spectral pattern was described of a peak in the spatial PSD_x located in the range of .11-.26 c/cm, which was broadly distributed in the temporal PSD_t. This pattern was described as the signature of a temporal impulse with a spatial period of 4-9 cm. The stripes that manifested the CAP could account for the temporal impulse. It was inferred that if phase cones and wave packets existed in human cortex, the diameters of the PM cones would be in the range of 2-4.5 cm, or about twice the diameter of the phase cones in rabbits. That size range served to predict that CAP would be found to occur on 6 to 15 contiguous electrodes at 3 mm spacing. The CAP were found in that range, but also in larger sizes up to the entire array, with less temporal spread than had been expected. This discrepancy suggested that the phase changes manifested in the

more widespread CAP stripes in scalp EEG might differ from those involved in forming wave packets in local areas of cortex.

3. Developments in techniques to search for AP differences

The definition and description of wave packets was based in behavioral correlation of the AM and PM patterns with behavior. The present preliminary study lacked an extensive behavioral data base. The technical problems to be solved were to devise optimal criteria by which to distinguish physiological phase jumps from those due to noise and artifacts, or to meaningless neural events resembling random avalanches in sand piles (Bak et al., 1987). Six procedures for interim optimization were examined here.

3.1. Unwrapping

First, four methods were explored for unwrapping: the MATLAB algorithm of adding a fixed correction at each branch point in time; an algorithm for locating zero crossings as an indicator of the need for a correction (Freeman and Rogers, 2000), estimation of when to add the required 2π offset with the atan2 algorithm; and estimation of when to add π with the atan algorithm. Of these the fourth procedure gave the smoothest ramp with the lowest number of outliers.

3.2. Band pass temporal filtering

Second, despite the 1/f form of the spectra of EEG and AA, narrow band pass filters were applied to the EEG prior to application of the Hilbert transform in search of the pass band of an optimal carrier frequency that might most clearly manifest state changes. In animals studies the pass band was evaluated by optimizing the classification of spatial AM patterns with respect to CS, giving species differences between cat and rabbit (Freeman, 2000a). Here the pass band was varied in search of CAP. As predicted, the mean of the distributions of AP differences depended on the center frequency of the pass band, and the variance depended on the band width. Spatial stripes of CAP were found in all of the files in at least some epochs, with varying spatial extents ranging from a few channels to the entire array. As expected, both forward and backward directions of AP differences across the array appeared within the same brief time periods. The clarity of the appearance of CAP was improved by display of the absolute values of the AP differences. Clarity improved with pass bands down to 20 Hz but was inadequate with those <10 Hz. This result was consistent with the finding that CAP occurred in different pass bands at different locations in time, indicating that they can coexist in the data, much as multiple phase cones were found to overlap in animal studies.

However, commonly within the same file there appeared stripes of CAP at differing times in different pass bands, particularly contrasting the beta and low gamma pass bands, so that multiple interleaved CAP were implied. This finding further raised the complex question, not yet answered, how subtle interactions between the narrow filters and the broad 1/f spectral distributions of the beta and gamma activity might give the appearance of distinctive, temporally interleaved markers for sequential state changes, or stages in the induction of each state change within a longer time window. Answers may require data taken at digitizing intervals of 1 or 2 ms instead of 5 ms as in the present study.

3.3. Use of minima in AA to clarify CAP

Third, unusually large increments in AP(t) differences tended to be accompanied by low values of AA, suggesting that a characteristic of cortical state changes was temporal amplitude modulation, by which at the AA tended to a minimum at the moment of a state

change. This finding was exploited by converting the AA(t) values from the filtered EEG signal to a weighting factor, W in equation (6), which approached zero for large AA and unity for small AA. Each AP difference was multiplied by the weight so as to diminish it between state changes and enhance it during state changes. This procedure enhanced the clarity of visual displays of the CAP. However, the variance of the relation between AA and AP was high, with numerous unexplained discrepancies in all directions, and, owing to the broad spatial distributions of mixed frequency components, the algorithm could not unequivocally distinguish AP jumps signifying state changes from those due to shifting low frequency base lines and the beats of oscillations in adjacent frequency bands.

3.4. Tuning curves to optimize the temporal pass band

Fourth, note was taken of the finding in files from occipital and paracentral areas that the interval between stripes was within the range of alpha wave durations. This finding was exploited by cross-correlating the unfiltered EEG with the AP differences after band pass filtering, computing the cospectrum, and finding the maximal peak in the alpha range, here 7.5 to 12.5 Hz. The procedure was repeated while systematically varying the upper and lower pass bands. The resulting tuning curves further enhanced the clarity of the CAP stripes across the array. Tuning curves were also used extensively in EEG studies of spatial AM patterns (Barrie, Freeman and Lenhart, 1996; Freeman, Gaál and Jörsten, 2003) and PM patterns (Freeman, 2003a).

However, the optimized pass band for the human AP(t) differences was in the beta range, not in the gamma range as had been predicted from the animal studies. The method for optimization of the pass band did not give sharp tuning curves in the absence of a detectable peak in the alpha range, and it was of little value for maximal power in the delta range, <3 Hz. There were too few files with PSD_t peaks in the theta and gamma ranges to support systematic investigation of the effects of varying the search range for the gating frequency outside the alpha range. Mesh plots of AP differences within the optimal beta band of 12 to 30 Hz from files with no alpha activity revealed stripes of CAP recurring aperiodically, indicating that AP stripes were not dependent on detectable alpha (Figure 19, A), as were the tuning curves. Other stripes recurring at alpha rates were equally prominent after temporal filtering to enhance the low gamma band, with or without alpha peaks in the PSD_t from unfiltered EEG (Figure 10, D).

3.5. Spatial low pass and high pass filtering

Fifth, the measurement of phase cones in EEG from subdural recording in animals was facilitated by low pass spatial filtering at 0.29 c/cm (Freeman and Barrie, 2000), and they were removed from the data by high pass filtering at 0.15 c/cm (Freeman and Baird, 1987). The results here replicated both the deleterious effect of high pass spatial filtering on the visualization of recurring stripes of CAP and the clarification of low pass filtering. Evaluation of the utility of spatial filtering was facilitated by over-sampling with a curvilinear array, with electrodes spaced 3 times more closely than the typical width of underlying gyri, conforming to the practical Nyquist criterion (Barlow, 1993). The combination of oversampling and smoothing appears to be optimal for spatial textural analysis (Freeman et al., 2003), however, the CAP phenomenon should also be accessible by means of the standard 10-20 clinical montage.

3.6. Comparison of resting state with intentional action

Sixth, the determination of an optimal pass band for application of the Hilbert transform to data from animals was based on a behavioral assay: the optimization of the classification of spatial AM patterns with respect to conditioned stimuli by varying the temporal band pass

filter. The carrier waves of the wave packets were found in the beta and gamma ranges of 20 to 80 Hz in rabbits (Barrie, Freeman and Lenhart, 1996) and 35-60 Hz in cats (Gaál and Freeman, 1998). In the present study the two behaviors were opening the eyes and intentionally adding EMG. Both actions were accompanied by tendencies of a temporal spectral peak to drop from the alpha range and sometimes for another to appear in the theta range. The spatial patterns of CAP stripes appeared to change in location and in detail, however, pattern analysis has not yet been undertaken. The clear visualization of CAP stripes in epochs when the EEG was overlain by EMG is strong evidence that the CAP are accessible in scalp EEG despite EMG. They are not wholly artifacts of data processing of aperiodic oscillations, because the PSD_t and PSD_x of EMG are broad and tend to be flat rather than 1/f (Freeman et al., 2003), indicating that EMG resembles white or colored noise and lacks the scaling properties of the EEG.

More study is needed, in particular to address the question whether the CAP stripes signify either idling of cortex, which is thought to occur during the relaxed awareness of traditional alpha states, or sequences of cognitive states, as manifested in EEG from intracranial electrode arrays in animals that yield AM patterns containing behaviorally related information, and that recur at rates in the theta and delta ranges. The best way to search the data is to extract the AM patterns from the EEG, map them in high dimensional state space, and classify them with respect to reproducible behaviors of subjects. A property of the AM patterns that facilitates classification is the fact the information content in the intracranial AM patterns is uniformly distributed over the channels. No channel is any more or less important than any other channel, as shown by deletion of randomly selected channels (Freeman and Baird, 1987, Figure 7; Barrie, Freeman and Lenhart, 1996, Figure 13; Ohl, Scheich and Freeman, 2001, Figure 3). This equivalence means that EEG data from sulci that is missing from scalp recordings may have no greater value for pattern classification than that from gyri that readily contributes to the scalp EEG, diminishing the need for intracranial recording. Animal studies indicate further that spatiotemporal patterns of AP have no utility for classification of EEG spatiotemporal patterns with respect to behavior, beyond serving as spatiotemporal markers of plateaus of AP(t) differences in which to search for AA(t) patterns.

Establishment of the behavioral correlates of changes in AA and AP will be necessary to answer the following question. Is the concentration in jumps of AP at times when the AA is low owing to loss of precision in the digitized data at low amplitudes, or can it be ascribed to a tendency for AA to go to a minimum at moments of phase change? No amount of signal processing can answer this question without reference to the possible cognitive content of the EEG.

4. Neural mechanisms of synchronization of jumps in CAP

The neural mechanisms of the CAP stripes remain open to speculation. The adverse effects of high pass spatial filtering and of re-referencing the data by subtracting the spatial ensemble average cannot be taken to show that the stripes are due to activity at the reference electrode or at a deep-lying generator. The stripes sometimes occupy the entire array (Figures 10, 13 and 16) but more often only a portion (Figures 14, 15 and 18), and the signed AP differences persist locally within the stripes, all with the same reference lead. This conclusion must be tempered by the realization that some as yet undetected sources of variation may exist in the multiple steps of data processing. The widespread synchrony may indicate the actions of neural mechanisms of global coordination, for which analysis of the timing will require a higher digitizing rate than the 200 Hz used here. An obvious candidate for coordination in and between hemispheres is control by thalamocortical projections (Hoppenstaedt and Izhkevich, 1998; Taylor, 1997; Steriade, 2000). The precision of timing might be consistent with the central location of the two thalamus, making

it roughly equidistant from the cortical areas underlying the locations of the array in this study. The low sampling rate of 200 Hz cannot support exploration, though it suffices to show that the AP differences do not occur as diagonal stripes, as might be expected from observations on phase lags in alpha activity across the vertex with magnetoencephalogram (Joliet, Ribary and Llinás, 1994), particularly with paracentral placements running anteroposteriorly.

The "zero phase lag" relations in the gamma range that are often reported in the literature present an even more difficult problem. A nominal limiting velocity of 10 m/s in cortex would suggest a maximal delay of 20 ms across the curvilinear array, corresponding to 4 digitizing time steps of 5 ms, which should have been commensurate with the temporal spread of CAP in this study, but a delay of 20 ms equals wave duration in the upper gamma range, and that is not compatible with a high degree of synchrony in the gamma range as widely reported (e.g., Singer and Gray, 1995; Haig, et al., 2000; Varela et al., 2001) and seen in spatial and temporal spectra from scalp EEG (Freeman et al., 2003).

5. Self-organized criticality and anomalous dispersion

An alternative theory by which to investigate cortical state changes is self-organized criticality (Bak, Tang and Wiesenfeld, 1987), in which the gyri, lobes, hemispheres and forebrain can be conceived as maintaining themselves in metastable states close to instability. The applicability of this theory to cortex is suggested by the 1/f form of the temporal and spatial spectra from the EEG, indicating power law scaling (Linkenkaer-Hansen et al., 2000; Hwa and Ferree, 2002; Freeman et al., 2003). The cortex is seething with changes in state occur simultaneously at all scales of time and space, ranging from those of single neurons through the mesoscopic states of wave packets to the entire forebrain. The possibility is that, while most of the state changes are local in time and space, some of them occasionally cascade into collections of coordinated wave packets and then into hemisphere-wide synchronized jumps in state, as revealed by CAP differences. The value of scalp recording emerges from the smoothing by the intervening soft and hard tissues, which attenuate the local states and enhance the appearance of the more extensive patterns of coordinated cortical activity. The larger scale patterns may be more likely to have correlates with cognitive functions than the local activity.

The apparent incompatibility of tight synchrony of gamma oscillations with axonal conduction delays (Freeman, 2000b) can be resolved by use of an analogy from optics, where a distinction is made between group or signal velocity and phase velocity in media that conduct light. The transmission of energy and information in all media can never exceed the speed of light, but when the frequency of the carrier light is close to an absorption or resonance band of a medium, the phase velocity can differ from and even appear to exceed the group velocity (Hecht and Zajac, 1974, p. 42 and p. 205). The light at the phase velocity manifests 'anomalous dispersion'.

The possibility of differing velocities in cortical dynamics first emerged through analysis of phase measurements of gamma activity in the olfactory bulb (Freeman, 1990). The phase velocity of the state change leading to AM pattern formation exceeded the velocity of serial synaptic transmission by a factor of about 20. This meant that the entire bulb transited from one state to another in ~5 ms, thereby keeping phase differences among gamma oscillations within the bulb under a quarter cycle of the carrier frequency. Previous measurements of the spread of activity evoked by electrical stimulation of the afferent pathway (Freeman, 1975) had demonstrated that serial synaptic transmission would require >100 ms to extend over the whole bulb. The proposed mechanism for the high phase velocity involved three factors. First, although the modal length of axon collaterals in the bulb is ~1 mm, a small percentage (~2-3%?) of axons extend for long distances under the

surface, or they cut through the white matter more directly. These long-range excitatory axons can sustain small world effects (Watts and Strogatz, 1998) that supplement local synaptic interactions. Second, if cortex by self-organizing criticality maintains itself at the edge of instability, then a small amount of coordinated activity may trigger a state change by which, for example, a sensory stimulus can destabilize a sensory cortex, causing it to jump from a state of expectancy to a state confirming one of several possible outcomes of search. The cascading state change by anomalous dispersion in bulb or neocortex could not carry information at a phase velocity exceeding the limiting velocity of group (serial synaptic) transmission, but it could trigger the selection and expression of previously stored information into spatial AM patterns of beta and gamma oscillations, with negligible time lags between widely separated areas. The trigger could be under thalamic control, but the actual coordination of the timing and content of beta and gamma oscillations, even over the entire extent of both cerebral hemispheres, could be an intrinsic property of the neocortex viewed as an integrated tissue. The question of the nature of a neural 'absorption" or "resonance" band in EEG spectra is interesting but too complex for consideration in the present context. It is dealt with elsewhere (Freeman and Rogers, 2003).

In the light of this line of thought the state change manifested in CAP differences may be equivalent to a phase transition in a physical system from a gas to a liquid. The beta and gamma oscillations that are detected at the scalp require coordinated activity of millions of neurons. The order parameter that they create and that 'enslaves' (Haken, 1999) their firing patterns must permeate throughout the populations. Suppose that a sensory stimulus excites the activity of a collection of feature detector neurons (Singer and Gray, 1995) forming a cloud of action potentials like molecules in a gas. The state change may be compared to condensation from a gas to a liquid. The entire population of synaptically connected neurons may transform its cloud of action potentials to an organized assembly, in which the structure manifested in the AM pattern derives from synaptic modifications with learning in prior experience, and the phase transition itself is manifested in the phase cone, comparable to the radial growth of a rain drop or snow flake from a site of nucleation at the apex (Freeman, 2000a). The read-out is by simultaneous broadcast of action potentials from all parts of the coordinated cortical populations by divergent axonal tracts that perform spatial integral transformations extracting the common mode activity (Freeman, 2003a; Freeman and Rogers, 2003). Control of the carrier frequency in the beta or gamma range need not be precise, provided that the initiating phase transition over the transmitting populations re-sets the phase of the carrier everywhere to the same starting value, and the window of transmission is kept brief. The role the CAP in this view would that of a synchronizing pulse, repeating sporadically without the precision of a clock, but with sufficient regularity, from time to time, to aggregate into the near-periodic oscillations seen in the theta and alpha ranges of the EEG and constituting an example of chaotic itinerancy (Tsuda, 2001).

Pursuit of theoretical analyses will require some advanced physics, as well as acquisition of scalp EEG data at finer temporal resolution from very high-density 2-D arrays, in conjunction with MRI display of the underlying gyri and sulci. Nonetheless, experimental studies of CAP stripes, intervening AM patterns, and their behavioral correlates can be done with equipment and expertise even now widely available in EEG clinics and teaching laboratories.

References

Bak P, Tang C, Wiesenfeld K. Self-organized criticality: an explanation of 1/f noise. Physical Review Letters 1987, 59: 364-374.

Barlow JS. The Electroencephalogram: Its Patterns and Origins. Cambridge MA: MIT Press, 1993.

Barrie JM, Freeman WJ, Lenhart M. Modulation by discriminative training of spatial patterns of gamma EEG amplitude and phase in neocortex of rabbits. J Neurophysiol 1996; 76: 520-539.

Bressler SL. Large-scale cortical networks and cognition. Brain Res. 1995, 20: 288-304.

Freeman WJ. On the problem of anomalous dispersion in chaoto-chaotic phase transitions of neural masses, and its significance for the management of perceptual information in brains. In: Haken H, Stadler M (eds.). Synergetics of Cognition. Berlin: Springer-Verlag, 1990, pp. 126-143.

Freeman WJ. Neurodynamics. An Exploration of Mesoscopic Brain Dynamics. London UK: Springer-Verlag, 2000a.

Freeman WJ. Characteristics of the synchronization of brain activity imposed by finite conduction velocities of axons. Intern. J. Bifurcation & Chaos 2000b 10: 2307-2322.

Freeman, W.J. [2003a] A neurobiological theory of meaning in perception. Part 1. Information and meaning in nonconvergent and nonlocal brain dynamics. Int. J. Bifurc. Chaos 13: 2493-2511.

Freeman, W.J. [2003b] A neurobiological theory of meaning in perception. Part 2. Spatial patterns of phase in gamma EEG from primary sensory cortices reveal the properties of mesoscopic wave packets. Int. J. Bifurc. Chaos 13: 2513-2535.

Freeman WJ, Baird B. Relation of olfactory EEG to behavior: Spatial analysis. Behav. Neurosci. 1987; 101: 393-408.

Freeman WJ, Barrie JM. Analysis of spatial patterns of phase in neocortical gamma EEG in rabbit. J. Neurophysiol. 2000; 84: 1266-1278.

Freeman, W.J. & Burke, B.C. [2003d] A neurobiological theory of meaning in perception. Part 4. Multicortical patterns of amplitude modulation in gamma EEG. Int. J. Bifurc. Chaos 13: 2857-2866.

Freeman, W.J., Gaál, G. & Jornten, R. [2003c] A neurobiological theory of meaning in perception. Part 3. Multiple cortical areas synchronize without loss of local autonomy. Int. J. Bifurc. Chaos 13: 2845-2856.

Freeman WJ, Grajski KA. Relation of olfactory EEG to behavior: Factor analysis: Behav. Neurosci. 1987; 101: 766-777.

Freeman, W.J., Burke, B.C., Holmes, M.D. & Vanhatalo, S. [2003] Spatial spectra of scalp EEG and EMG from awake humans. Clin. Neurophysiol. 114: 1055-1060.

Freeman WJ, Rogers LJ. Fine temporal resolution of analytic phase reveals episodic synchronization by state transitions in gamma EEG. J. Neurophysiol. 2002; 87: 937-945.

Freeman, W.J. & Rogers, L.J. [2003e] A neurobiological theory of meaning in perception. Part 5. Multicortical patterns of phase modulation in gamma EEG. Int. J. Bifurc. Chaos 13: 2867-2887.

Freeman WJ, Rogers LJ, Holmes MD, Silbergeld DL. Spatial spectral analysis of human electrocorticograms including the alpha and gamma bands. J. Neurosci. Meth. 2000, 95: 111-121.

Freeman WJ, Van Dijk B. Spatial patterns of visual cortical fast EEG during conditioned reflex in a rhesus monkey. Brain Res. 1987; 422: 267-276.

Freeman WJ, Viana Di Prisco G. Relation of olfactory EEG to behavior: Time series analysis. Behav. Neurosci. 1986; 100: 753-763.

Gaál G, Freeman WJ. Relations among EEGs from entorhinal cortex, olfactory bulb, somatomotor, auditory and visual cortices in trained cats. In: Ding M, Ditto W, Pecora L,

Spano M, Vohra S (eds.) Proc. 4th Exp. Chaos Conf. Singapore: World Scientific, pp. 179-184.
Gonzalez RC, Wintz P (1977) Digital Image Processing. Reading MA: Addison-Wesley.
Haig AR, Gordon E, Wright JJ, Meares RA, Bahramali H. Synchronous cortical gamma-band activity in task-relevant cognition. NeuroReport 2000;11: 669-675.
Haken, H. What can synergetics contribute to the understanding of brain functioning? In: Analysis of Neurophysiological Brain Functioning. Uhl, C, (ed.) Berlin: Springer-Verlag, 1999. pp. 7-40.
Hecht E, Zajac A. Optics. Reading MA: Addison-Wesley Publ., 1974, pp. 38-42, 205-205.
Hoppensteadt, FC and Izhkevich, EM. Thalamo-cortical interactions modeled by weakly connected oscillators: could the brain use FM radio principles? BioSystems 1998, **48**: 85-94.
Hwa RC, Ferree T. Scaling properties of fluctuations in the human electroencephalogram. Physical Rev 2002; E 66: 021901.
Ingber L. Statistical mechanics of multiple scales of neocortical interactions. In: Nunez PL, Neocortical Dynamics and Human EEG Rhythms. New York NY: Oxford University Press 1995, pp. 628-681.
Joliot M, Ribary U, Llinás R. Human oscillatory brain activity near 40 Hz coexists with cognitive temporal binding. Proc. Nat. Acad. Sci. USA 1994; 91: 11748-11751.
Lachaux J P, Rodriguez E, Martinerie J, Varela J. Measuring phase synchrony in brain signals. Human Brain Mapping 1999; 9:194-208.
Le Van Quyen M, Foucher J, Lachaux J-P, Rodriguez E, Lutz A, Martinerie J and Varela F. Comparison of Hilbert transform and wavelet methods for the analysis of neuronal synchrony. J. Neurosci. Meth. 2001, 111: 83-98.
Linkenkaer-Hansen K, Nikouline VM, Palva JM, Ilmoniemi RJ. Long-range temporal correlations and scaling behavior in human brain oscillations. J. Neurosci. 2001; 15: 1370-1377.
Miltner WHR, Barun C, Arnold M, Witte H, Taub E. Coherence of gamma-band EEG activity as a basis for associative learning. Nature 1999; 397: 434-436.
Müller MM. Hochfrequente oszillatorische Aktivitäten im menschlichen Gehirn. Zeitschrift f. Exper. Psychol. 2000; 47: 231-252.
Müller MM, Bosch J, Elbert T, Kreiter A, Valdes Sosa M, Valdes Sosa P, Rockstroh B. Visually induced gamma band responses in human EEG - A link to animal studies. Exper. Brain Res. 1996;112:96-112.
Nunez PL, Srinivasan R, Westdorp AF, Wijesinghe RS, Tucker DM, Silberstein RB, Cadusch PJ. EEG coherency I: statistics, reference electrode, volume conduction, Laplacians, cortical imaging and interpretation at multiple scales. Electroenceph. clin. Neurophysiol. 1997, 103: 499-515.
Ohl FW, Scheich H, Freeman WJ. Change in pattern of ongoing cortical activity with auditory category learning. Nature 2001; 412: 733-736.
Pikovsky A, Rosenblum M, Kurths J. Synchronization — A Universal Concept in Non-linear Sciences. Cambridge UK: Cambridge University Press, 2001.
Quiroga R, Kraskov A, Kreuz T and Grassberger P. Performance of different synchronization measures in real data: A case study on electroencephalographic signals. Phys. Rev. E 2002, 65: 041903.
Rodriguez E, George N, Lachaux J-P, Martinerie J, Renault B, Varela F. Perception's shadow: long-distance synchronization of human brain activity. Nature 1999; 397: 430-433.
Singer W, Gray CM. Visual feature integration and the temporal correlation hypothesis. Ann . Rev. Neurosci. 1995, 18: 555-586.
Steriade, M. Corticothalamic resonance, states of vigilance, and mentation. Neuroscience 2000, 101: 243-276.

Tallon-Baudry C, Bertrand O, Delpuech C, Pernier J. Stimulus-specificity of phase-locked and non phase-locked 40-Hz visual responses in human. J. Neurosci 1996; 16: 4240-4249.

Tallon-Baudry C, Bertrand O, Peronnet F, Pernier J. Induced gamma-band activity during the delay of a visual short-term memory task in humans. J. Neurosci. 1998; 18: 4244-4254.

Tass P, Kurths J, Rosenblum M, Weule J, Pikovsky A, Volkmann J, Schnitzler H, Freund H Complex phase synchronization in neurophysiological data. In: Analysis of Neurophysiological Brain Functioning. Uhl, C. (ed.), Berlin: Springer-Verlag, 1999, pp. 252-273.

Taylor, JG. Neural networks for consciousness. Neural Networks 1997, 10: 1207-1225.

Tsuda, I. Toward an interpretation of dynamics neural activity in terms of chaotic dynamical systems. Behav. & Brain Sci. 2001, 24: 793-847.

Varela F, Lachaux J-P, Rodriguez E and Martinerie J (2001) The brainweb: Phase synchronization and large-scale integration. Nature Reviews Neurosci. 21: 229-239.

Watts, DJ and Strogatz, SH. Collective dynamics of 'small world' networks. Nature 1998, 394: 440-442.